CAPITAL UNIVERSITY OF SCIENCE AND TECHNOLOGY, ISLAMABAD

Thermal Radiation and MHD Stagnation Point Flow of Micropolar Fluid over a Shrinking Sheet

by

Kamran Khan

A thesis submitted in partial fulfillment for the degree of Master of Science

in the

Faculty of Computing
Department of Mathematics

2018

I would like to dedicate my thesis to my beloved parents

CAPITAL UNIVERSITY OF SCIENCE & TECHNOLOGY

ISLAMABAD

CERTIFICATE OF APPROVAL

Thermal Radiation and MHD Stagnation Point Flow of Micropolar Fluid over a Shrinking Sheet

by

Kamran Khan

MMT161013

THESIS EXAMINING COMMITTEE

S. No.	Examiner	Name	Organization
(a)	External Examiner	Dr. Tanvir Akbar Kiani	COMSATS university, Islamabad
(b)	Internal Examiner	Dr. Shafqat Hussain	CUST Islamabad
(c)	Supervisor	Dr. Muhammad Sagheer	CUST Islamabad

Thesis Supervisor
Dr. Muhammad Sagheer
November, 2018

Dr. Muhammad Sagheer
Head
Dept. of Mathematics
November, 2018

Dr. Muhammad Abdul Qadir
Dean
Faculty of Computing
November, 2018

Author's Declaration

I, **Kamran Khan** hereby state that my M. Phil thesis titled "**Thermal Radiation and MHD Stagnation Point Flow of Micropolar Fluid over a Shrinking Sheet**" is my own work and has not been submitted previously by me for taking any degree from Capital University of Science and Technology, Islamabad or anywhere else in the country/abroad.

At any time if my statement is found to be incorrect even after my graduation, the University has the right to withdraw my M. Phil Degree.

(Kamran Khan)

Registration No: MMT161013

Plagiarism Undertaking

I solemnly declare that research work presented in this thesis titled "**Thermal Radiation and MHD Stagnation Point Flow of Micropolar Fluid over a Shrinking Sheet**" is solely my research work with no significant contribution from any other person. Small contribution/help wherever taken has been dully acknowledged and that complete thesis has been written by me.

I understand the zero tolerance policy of the HEC and Capital University of Science and Technology towards plagiarism. Therefore, I as an author of the above titled thesis declare that no portion of my thesis has been plagiarized and any material used as reference is properly referred/cited.

I undertake that if I am found guilty of any formal plagiarism in the above titled thesis even after award of M. Phil Degree, the University reserves the right to withdraw/revoke my M. Phil degree and that HEC and the University have the right to publish my name on the HEC/University website on which names of students are placed who submitted plagiarized work.

(Kamran Khan)

Registration No: MMT161013

Acknowledgements

First and foremost I would like to pay my cordial gratitude to the Almighty **Allah**, Who created us as a human being with the great boon of intellect. I would like to pay my humble gratitude to the Allah Almighty, for blessing us with the Holy Prophet **Hazrat Muhammad (Sallallahu Alaihay Wa'alihi wasalam)** for whom the whole universe is being created. He (Sallallahu Alaihay Wa'alihi wasalam) removed the ignorance from the society and brought us out of darkness. Thanks again to that Monorealistic Power for granting me with a strength and courage whereby I dedicately completed my MS thesis with positive and significant result.

I owe honour, reverence and indebtedness to my accomplished supervisor and mentor **Dr. Muhammad Sagheer** whose affectionate guidance, authentic supervision, keen interest and ingenuity was a source of inspiration for commencement, advancement and completion of the present study. I would like to acknowledge CUST to providing me such a favourable environment to conduct this research. My especial thanks to **Maleeha Atlas** and **Dr. Muhammad Bilal** for his inspiring guidance and untiring help during the research period.

Thanks to my best friend **M. Yamin** for her ever encouragement and overall support during my entire university life.
It will be injustice if I forget my beloved parents, brothers and kind persons. Thanks to my father **Safdar Khan**, my great uncle **Khani Zaman**, brothers **Qaisar Zaman**, **Johar Zaman** and **Hamza Khan** for their ever encouragement and overall support during my entire university life. May Almighty Allah shower his blessings and prosperity on all those who assisted me during the completion of this thesis.

Abstract

In this thesis, we study the micropolar fluid stagnation point flow over a stretching/shrinking sheet with the second order velocity slip. Thermal radiation and MHD stagnation point flow of a micropolar fluid over a shrinking sheet is investigated. The assumptions on the micropolar fluid flow are that two-dimensional, steady, laminar and incompressible. The similarity transformation is used to convert the partial differential equations (PDEs) into the ordinary differential equations (ODEs). The numerical results have been found by the shooting technique. The effect of different parameters such as the micropolar parameter, the magnetic field, Prandtl number, aligned angle of magnetic field, 2nd order slip, stretching/shrinking rate, first order slip , suction parameter and thermal radiation on the velocity, microrotation and temperature profiles are analyzed through tables and graphs.

Contents

List of Figures

List of Tables

Symbols

(u, v)	velocity components	$u_w(x)$	stretching/shrinking velocity
ρ	fluid density	N	component of microrotation
η	similarity variable	T_∞	ambient temperature
μ	dynamic viscosity	Nu_x	local Nusselt number
k	microrotation viscosity	T_0	reference temperature
j	microinertia density	q_w	surface heat flux
x	horizontal coordinate	C_{fx}	skin friction in x-direction
y	vertical coordinate	Re_x	local Reynold number
σ	electrical conductivity	ψ	stream function
$u_e(x)$	free stream velocity	h	dimensionless micro-rotation
M	magnetic field	f	dimensionless velocity
K	micropolar parameter	$f''(0)$	skin friction coefficient
q_r	radiative heat flux	θ	dimensionless temperature
λ	first order slip	ϵ	stretching/shrinking rate
T	fluid temperature	σ^*	Stefan Boltzman constant
δ	second order slip	α	aligned angle of magnetic field
λ_1	suction/injection	C_p	specific heat
Pr	Prandtl number	T_w	wall temperature
R_d	thermal radiation	τ_w	surface shear stress
α_1	thermal diffusivity	n	microrotation parameter

Chapter 1

Introduction

The study of fluid on the stretching sheet is an important problem which has been discussed in the current era because of its importance in different processes of engineering like manufacturing processes such as glass fiber drawing, paper production and plastic extrusion by Thomason *et al.* [1]. The fluid mechanics deals with the behaviour of fluids at rest and in motions. Zheng *et al.* [2] investigated the temperature effect with velocity slip on magnetohydrodynamics flow and heat transfer over a shrinking sheet. Sakiadis [3] was the first one who investigated the boundary layer flow on a continuous solid surface moving at a constant speed. Ishak *et al.* [4] extended the Blasius and Sakiadis equations. Stagnation point is a point in a flow field which has zero fluid's velocity. The stagnation point flows are of considerable importance in the fluid dynamic field and have been investigated by many researchers. Hiemenz [5] was the first one who investigated the stagnation point flow due to stretching sheet. Eckert [6] extanded Hiemenz' work [5] along with the energy equation. Zaimi and Ishak [7] investigated the slip effect on heat transfer and stagnation point flow due to stretching vertical sheet. Fauzi *et al.* [8] investigated the slip effect on the steady stagnation point flow and heat transfer due to shrinking rate in a viscous fluid. Bhattacharyya *et al.* [9] discussed the slip effect on the heat transfer and stagnation point flow over a shrinking sheet.

Many researchers found interested in the study of the micropolar fluid for the different geometries. Erigen [10] was the first one who investigated the micropolar

fluid. Ariman *et al.* [11] theoretically investigated the micropolar fluids and their applications. Ishak *et al.* [12] discussed the stagnation point flow of a micropolar fluid in two dimensional boundary layer flow of mixed convection on a stretching sheet. Bhargava *et al.* [13] numerically investigated the solutions of micro-polar transport due to a non-linear stretching sheet. Rees and Pop [14] theoretically discussed free convection from a vertical flat plate in a micropolar fluid. Nazar *et al.* [15], Ishak *et al.* [16], Hayat *et al.* [17], Yacob *et al.* [18] have also discussed the stagnation point flow of a micropolar fluid due to stretching sheet, under different physical conditions.

The effect of slip condition gives an interesting results for different fluids. Dorrepaal [19] was the first one who introduced the slip velocity effect. Bellani and Variano [20] discussed the slip velocity effect on the turbulent flow. Wang [21] studied the slip effect on the viscous flow due to a stretching sheet. Noghrehabadi *et al.* [22] investigated the partial slip effect on the heat transfer of nano-fluids over a stretching sheet. Sharma *et al.* [23] investigated the slip effect of the heat transfer due to stretching sheet on a CuO- water nano-fluid. A new model effect of second order slip velocity was introduced by Wu [24]. Wang *et al.* [25] extended the article of Wu [24] by considering the slip effect of stagnation point flow on a heated vertical plate. Fang *et al.* [26] investigated the second order velocity slip effect on the viscous flow due to a stretching sheet. Nandeppanaver *et al.* [27] discussed the heat transfer and second order slip flow due to a stretching sheet. Deissler [28], Roşca and Pop [29] and Turkyilmazoglu [30] investigated the second order velocity slip effect, under different physical conditions.

The study of magnetic properties of electrically conducting fluids is known as Magnetohydrodynamics (MHD). Many researchers are interested in the study of MHD fluid flow because of its important applications in the processes of engineering. Alfven [31] was the first who introduced the effect of MHD on fluids flow. Yih [32] numerically investigated the heat and mass transfer of free convection effect on magnetohydrodynamic of a continuously moving permeable vertical surface. Zheng *et al.* [33] discussed the MHD flow and heat transfer over a porous shrinking sheet with temperature jump and velocity slip.

Radiation is a process by which the heat is transferred through the electromagnetic waves and it is the only heat transfer process that does not require a medium (i.e. molecules) to transfer energy from a hot to a cold region. Makinde *et al.* [34] investigated the thermal radiation effect on the heat and mass transfer flow of a variable viscosity fluid. The thermal radiation effect on MHD nanofluid between two horizontal rotating plates was analysed by Sheikholeslami *et al.* [35]. Raptis *et al* [36] and Arpaci [37] discussed the effect of thermal radiation under different physical conditions.

1.1 Thesis Contribution

In this thesis, a review study of Sharma *et al.* [38] has been presented and then the flow analysis has been extended by considering the thermal radiation and aligned magnetic field. The similarity transformation is used to transform the modeled PDEs into a system of ODEs. The numerical results have been found by the shooting technique and compared with those obtained through the MATLAB built-in solver bvp4c. The numerical results are analyzed for behaviour of different parameters through tables and graphs.

1.2 Thesis Outline

This thesis is further arranged in the following order:
In **Chapter 2**, some basic definitions and terminologies of the fluid and relevant material are presented.

Chapter 3 contains a detailed review of the article of Sharma *at el.* [38]. A numerical study of incompressible micropolar fluid, laminar, two-dimensional, stagnation point, slip flow over a stretching/shrinking sheet has been examined.

In **Chapter 4** the work of Sharma *at el.* [38] is extended by including the thermal radiation and aligned magnetic field. Numerical values of the Nusselt number and

skin friction coefficient have also been computed and discussed in this chapter. Tables and graphs describe the behaviour of different physical parameters.

Chapter 5 summarizes the whole research work and gives recommendations for future work.

All the references used in the research work are listed in **Bibliography**.

Chapter 2

Some Basic Definitions and Governing Equations

In this chapter, some basic definitions, fundamental concepts and ideas of fluid dynamics have been included. The terminologies relevant to the rest of the thesis have been specially focused. Most of these have been taken from [39].

2.1 Fluid

"Fluid is a material which has the ability to flow. Both liquids and gases are termed as fluids."

2.2 Fluid Dynamics

"The study of fluids and its characteristics at motion."

2.3 Pressure

"The ratio of applied force to the unit area is said to be pressure. It is represented by P and mathematically, written as

$$P = \frac{F}{A}, \tag{2.1}$$

where A and F denote the unit area and the applied force, respectively."

2.4 Density

"The mass per unit volume of a material is known as its density. Symbolically, it is denoted by ρ and mathematically, it is expressed as

$$\rho = \frac{m}{v}, \tag{2.2}$$

where v and m are the volume and mass of the material, respectively."

2.5 Stress

"Stress is the force acting on the surface of the unit area within the distortable body. Mathematically,

$$\rho = \frac{F}{A}, \tag{2.3}$$

where A is the area and F is the force."

2.6 Normal Stress

"Normal stress is the element of stress in which a force acts normal to the unit surface area."

2.7 Kinematic Viscosity

"The ratio between the dynamic density and viscosity is defined as the kinematic viscosity and is denoted by ν:

$$\text{Kinematic viscosity} = \frac{\text{dynamic viscosity}}{\text{dynamic density}} \tag{2.4}$$

$$\text{or} \quad \nu = \frac{\mu}{\rho}." \tag{2.5}$$

2.8 Classification of Fluids

2.8.1 Ideal Fluid

"Those fluids which have zero viscosity, are called ideal fluids."

2.8.2 Real Fluid

"A fluid is said to a real fluid if it has a non-zero viscosity."

2.8.3 Newton's Law of Viscosity

"The shear stress which distorts the fluid components viscosity is directly and linearly proportional to the velocity gradient. Mathematically,

$$\tau_{yx} \propto \frac{du}{dy},$$

$$\text{or} \quad \tau_{yx} = \mu \frac{du}{dy}, \tag{2.6}$$

where τ_{yx} is the shear stress component of the fluid, u is the component of the velocity and μ is the viscosity proportionality constant."

2.8.4 Newtonian Fluids

"The real fluids for which the shear stress of the fluid varies directly and linearly as the deformation rate, are called Newtonian fluids. Mathematically,

$$\tau_{yx} = \mu \frac{du}{dy}, \tag{2.7}$$

where τ_{yx} is the shear stress, u denotes x-component of velocity and μ denotes dynamic viscosity. Examples of Newtonian fluids are water, air, oxygen gas and silicone oil etc."

2.8.5 Non-Newtonian Fluids

"Non-Newtonian fluids are those for which the shear stress is not linearly proportional to the deformation rate. Mathematically, it can be written as

$$\tau_{yx} \propto \left(\frac{du}{dy}\right)^m, \ m \neq 1$$

$$\text{or} \quad \tau_{yx} = \mu \left(\frac{du}{dy}\right)^m, \tag{2.8}$$

where μ denotes the viscosity, m is the index of flow performance. Note that for $m = 1$, the above equation (2.8) reduces to the Newton's law of viscosity. Blood, paint, shampoo, toothpaste are the examples of non-Newtonian fluids."

2.9 Types of Flow

2.9.1 Turbulent Flow

"In turbulent flow, the motion of the fluid particles is irregular and the path lines are the erratic curves."

2.9.2 Uniform Flow

"If the velocity of the flow has the same magnitude and direction during the motion of a fluid, then the flow is said to be a uniform flow. Mathematically, it can be written as

$$\frac{dV}{ds} = 0, \tag{2.9}$$

where V is the velocity and s is the displacement in any direction."

2.9.3 Non-Uniform Flow

"In a non-uniform flow, the velocity is not same at every point of the fluid at a given instant. Mathematically, it is expressed as

$$\frac{dV}{ds} \neq 0, \tag{2.10}$$

where V is the velocity and s is the displacement."

2.9.4 Internal Flow

"The flow bounded by a solid surface is known as an internal flow. An example of the internal flow is the flow in pipe or duct."

2.9.5 External Flow

"The flow, which is not bounded by a solid surface, is known as an external flow. An example of the external flow is the water-flow in the river or in the ocean."

2.9.6 Steady Flow

"The flow, which is independent of time is said to be a steady flow. Mathematically, it can be written as

$$\frac{d\xi}{dt} = 0, \tag{2.11}$$

where ξ is any fluid property."

2.9.7 Unsteady Flow

"The flow, which depends on time, is known as unsteady flow. Mathematically, it can be written as

$$\frac{d\xi}{dt} \neq 0, \tag{2.12}$$

where ξ is any fluid property."

2.9.8 Compressible Flow

"The fluid flow in which the density with respect to the substance is not constant is said to be a compressible flow." Mathematically, it is expressed by

$$\rho(x, y, z, t) \neq c, \tag{2.13}$$

where c is a constant."

2.9.9 Incompressible Flow

"The flow of fluid in which the density is constant, is said to be an incompressible flow. It is mathematically described by

$$\rho(x, y, z, t) = c, \tag{2.14}$$

where c is a constant."

2.10 Heat Transfer Modes

2.10.1 Conduction

"The flow of heat through a solid or liquid by the intersection of free electrons and molecules is said to be conduction. In other words, the heat transfer from one body to another due to the molecular agitation with a material without any motion of the material as whole is called conduction. Mathematically, it can be written as

$$q = -kA\left(\frac{\Delta T}{\Delta n}\right), \tag{2.15}$$

where k and $\frac{\Delta T}{\Delta n}$ denote the constant of the thermal conductivity and gradient of the temperature respectively."

2.10.2 Convection

"In this process, heat transfer occurs due to the bulk fluid motion of molecules or transfer of molecules. Mathematically, it is expressed as

$$q = hA(T_s - T_\infty), \tag{2.16}$$

where h, A, T_s and T_∞ denote the heat transfer coefficient, the area, the temperature of the surface and the temperature away from the surface respectively."

2.10.3 Mixed Convection

"Mixed convection is a mechanism in which both free and forced convection process simultaneously and significantly contribute to transfer the heat."

2.10.4 Radiation

"Radiation is the emission of energy in the form of waves or particles. For example, if we place a material object (e.g, a piece of steel) under the sun rays, after a few moments, we observe that the material object is heated. Such phenomenon takes place due to radiation. Mathematically, it can be written as

$$q = E\sigma A[(\Delta T)^4], \tag{2.17}$$

where E, σ, ΔT, A, q are the emissivity of the scheme, the constant of Stephan-Boltzmann ($5.670 \times 10^-8 \frac{W}{m^2 K^4}$), the variation of the temperature, the area and the amount of heat transferred respectively."

2.11 Dimensionless Numbers

2.11.1 Prandtl Number

"The ratio of the kinematic diffusivity to the thermal diffusivity is said to be the Prandtl number. It is denoted by Pr and mathematically it can be written as

$$Pr = \frac{\nu}{\alpha} = \frac{\frac{\mu}{\rho}}{\frac{k}{\rho c_p}} = \frac{\mu c_p}{k}, \tag{2.18}$$

where ν, α denote the momentum diffusivity or kinematic diffusivity and the thermal diffusivity respectively. Physical significance of Prandtl number is that it gives the respective thickness of the velocity boundary layer and the thermal boundary layer. For small Pr, heat diffuses very quickly as compared to the momentum."

2.11.2 Nusselt Number

"It examines the ratio of convective to the conductive heat transfer through the boundary of the surface. It is a dimensionless number which was first introduced by the German mathematician Nusselt. Mathematically, it is expressed by

$$Nu = \frac{h\Delta T}{\frac{k\Delta T}{\delta}} = \frac{h\delta}{k}, \tag{2.19}$$

where h, δ and k denote the coefficient of heat transfer, the characteristic length and the thermal conductivity respectively."

2.12 Basic Laws

2.12.1 Law of Conservation of Mass

"Continuity equation is derived from the law of conservation of mass and mathematically, it is expressed by

$$\frac{\partial \rho}{\partial t} + \nabla.(\rho V) = 0, \tag{2.20}$$

where t is the time. In case of an incompressible fluid, the continuity equation is expressed by

$$\nabla.V = 0." \tag{2.21}$$

2.12.2 Law of Conservation of Energy

"The energy equation for the fluid is

$$\rho C_p(\frac{\partial}{\partial t} + V\nabla)T = k\nabla^2 T + \tau L + \rho C_p\left[D_B \nabla C.\nabla T + \frac{D_T}{T_m}\nabla T\right], \tag{2.22}$$

where $(C_p)_f$ denotes the specific heat of the basic fluid, the specific heat of the material has been represented by $(C_p)_s$, the density of basic fluid by ρ_f, the rate of strain tensor represented by L, the temperature of the fluid represented by T, the Brownian motion coefficient by D_B the , the temperature diffusion coefficient by D_T and the mean temperature by T_m. The expression for Cauchy stress tensor for viscous incompressible fluid is expressed by

$$\tau = -pI + \mu A_1. \tag{2.23}$$

In above equation tensor has been represented by A_1, pressure represented by p and the dynamic viscosity by μ.

$$A_1 = \nabla V + (\nabla V)^t, \tag{2.24}$$

where $(\ )^t$ represents transpose of the matrix for two dimensional field velocity of the fluid. The stain tensor τ can be written as

$$\tau = \begin{pmatrix} \sigma_{xx} & \tau_{yx} & \tau_{zx} \\ \tau_{xy} & \sigma_{yy} & \tau_{zy} \\ \tau_{xz} & \tau_{yz} & \sigma_{zz} \end{pmatrix}." \tag{2.25}$$

2.13 Methodology

"Shooting method is a numerical technique used to solve the boundary value problems for non-linear coupled ordinary differential equations. In this technique to convert the boundary value problems into initial value problems. The differential equations of initial value problems are integrated numerically through RK-4 method. The formulated problem needs the IVP with arbitrarily chosen initial conditions to approximate the boundary conditions. If the boundary conditions are not fulfilled to the required accuracy, with the new set of initial conditions, which are modified by Newton's method. The process of Newton method is repeated until the require accuracy. Consider, the second order boundary value problem,

$$y'' = f(x, y, y'), \tag{2.26}$$

along with boundary conditions

$$y(0) = 0, \quad y(A) = B. \tag{2.27}$$

To have a system of first order ODEs, use the notations:

$$y = y_1, \quad y' = y_2. \tag{2.28}$$

By using the notations (2.28) in (2.26) and (2.27) can be written as

$$\left.\begin{aligned} y_1' &= y_2, \quad y_1(0) = 0, \\ y_2' &= f(x, y_1, y_2), \quad y_1(A) = B. \end{aligned}\right\} \tag{2.29}$$

Choose the missing initial condition $y_2(0) = g$, we have the following IVP:

$$\left.\begin{aligned} y_1' &= y_2, \quad y_1(0) = 0, \\ y_2' &= f(x, y_1, y_2), \quad y_2(0) = g. \end{aligned}\right\} \tag{2.30}$$

Now, the initial value problem satisfy the boundary condition $y_2(A) = B$,

$$y_1(A, g) - B = \phi(g) = 0, \tag{2.31}$$

To find an approximate root of (2.31) by the Newton's method, is written as

$$g_{n+1} = g_n - \frac{\phi(g_n)}{\phi'(g_n)} \tag{2.32}$$

or

$$g_{n+1} = g_n - \frac{y_1(A, g_n) - B}{\frac{\partial}{\partial g}[y_1(A, g_n) - B]} \tag{2.33}$$

To implement the Newton's scheme, consider the following notations:

$$\frac{\partial y_1}{\partial g} = y_3, \quad \frac{\partial y_2}{\partial g} = y_4 \tag{2.34}$$

Differentiating equations (2.30) *w.r.t.* g, we get the following four first order ODEs along with the associated initial conditions.

$$\left.\begin{aligned} y_3' &= y_4, \quad y_3(0) = 0, \\ y_4' &= y_3 \frac{\partial f}{\partial y_1} + y_4 \frac{\partial f}{\partial y_2}, \quad y_4(0) = 1. \end{aligned}\right\} \tag{2.35}$$

Now, solving the IVP (2.35), we get y_3 at A. This value is actually the derivative of y_1 with respect to g computed at A. Using the value of $y_3(A, g)$ in Eq. (2.33),

the modified value of g can be achieved. This new value of g is used to solve the Eq. (2.30) and the process is repeated until the require accuracy."

Chapter 3

Stagnation Point Flow of Micropolar Fluid over a Stretching/Shrinking Sheet

3.1 Introduction

In present chapter, we provided a detailed review of [38] has been presented. The stagnation point flow of a micropolar fluid on a stretching/shrinking sheet has been discussed subject to the assumption of velocity slip. The similarity transformation is used to transform the modeled PDEs into a system of ODEs. The numerical results have been found by the shooting method. Finally, the numerical results are presented with discussion of the effects of different physical parameters.

3.2 Mathematical Modeling

Consider a steady, two-dimensional stagnation point flow of an incompressible micropolar fluid on a stretching/shrinking sheet with the assumption of slip velocity effect. Assume that $u_e(x) = ax$ be the free stream velocity and $u_w(x) = bx$ be the stretching/shrinking velocity respectively, where a and b are some real constants.

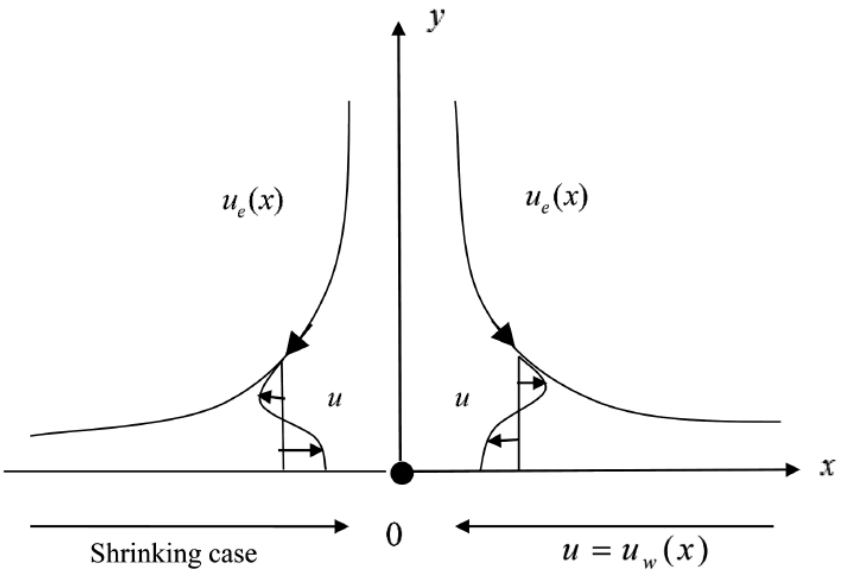

Figure 1: Geometry of the problem.

For stretching sheet $b > 0$ and for shrinking sheet $b < 0$. The mathematical model of the flow, presented by Sharma *et al.* [38] is as follows:

$$\frac{\partial u}{\partial x} + \frac{\partial v}{\partial y} = 0, \tag{3.1}$$

$$u\frac{\partial u}{\partial x} + v\frac{\partial u}{\partial y} = u_e\frac{\partial u_e}{\partial x} + \left(\frac{\mu + k}{\rho}\right)\frac{\partial^2 u}{\partial y^2} + \frac{k}{\rho}\frac{\partial N}{\partial y}, \tag{3.2}$$

$$\rho j\left(u\frac{\partial N}{\partial x} + v\frac{\partial N}{\partial y}\right) = \left(\mu + \frac{k}{2}\right)j\frac{\partial^2 N}{\partial y^2} - k\left(2N + \frac{\partial u}{\partial y}\right), \tag{3.3}$$

where the velocity components has been represented by u and v respectively. Dynamic viscosity is denoted by μ, microrotation viscosity by k, fluid density by ρ, micro inertia density by j and component of microrotation is denoted by N. The boundary conditions of the above equations are given as

$$\left.\begin{aligned} &v = 0, \quad u = u_{slip} + u_w(x), \quad N = -n\frac{\partial u}{\partial y} \quad at\ y = 0, \\ &u \to u_e(x), \quad N \to 0 \quad as\ y \to \infty, \end{aligned}\right\} \tag{3.4}$$

where $u_e(x)$, u_{slip} and $u_w(x)$ represent the free steam velocity, slip velocity and stectching/shrinking velocity. The stream function ψ identically satisfies the continuity equation. Mathematically,

$$u = \frac{\partial \psi}{\partial y}, \qquad v = -\frac{\partial \psi}{\partial x}. \tag{3.5}$$

Now, introduce the following similarity variables from [38],

$$\left.\begin{aligned} \psi &= \sqrt{\nu x u_e(x)} f(\eta) = \sqrt{a\nu} x f(\eta), \\ \eta &= \sqrt{\frac{u_e(x)}{\nu x}} y = \sqrt{\frac{a}{\nu}} y, \\ N &= u_e(x) \sqrt{\frac{u_e(x)}{\nu x}} h(\eta) = a\sqrt{\frac{a}{\nu}} x h(\eta), \end{aligned}\right\} \tag{3.6}$$

where the stream function is represented by ψ and the kinematic viscosity is represented by ν.

$$\left.\begin{aligned} &\bullet\ u = \frac{\partial}{\partial y}\left(\sqrt{a\nu} x f(\eta)\right) = \sqrt{a\nu} x f'(\eta) \frac{\partial \eta}{\partial y} = a x f'(\eta) \\ &\bullet\ v = -\frac{\partial}{\partial x}\left(\sqrt{a\nu} x f(\eta)\right) = -\sqrt{a\nu} f(\eta) \end{aligned}\right\} \tag{3.7}$$

$$\left.\begin{aligned} &\bullet\ \frac{\partial u}{\partial x} = \frac{\partial}{\partial x}\left(a x f'(\eta)\right) = a f'(\eta) \quad \left(\because\ \eta = \sqrt{\frac{a}{\nu}} y\right) \\ &\bullet\ \frac{\partial v}{\partial y} = \frac{\partial}{\partial y}(-\sqrt{a\nu} f(\eta)) = -\sqrt{\nu a} f'(\eta) \frac{\partial \eta}{\partial y} = -a f'(\eta) \end{aligned}\right\} \tag{3.8}$$

Looking at (3.8), the continuity Eq. (3.1) is straight forwardly satisfied.

$$\left.\begin{aligned} &\bullet\ \frac{\partial u}{\partial y} = \frac{\partial}{\partial y}\left(a x f'(\eta)\right) = a x f''(\eta) \frac{\partial \eta}{\partial y} = a\sqrt{\frac{a}{\nu}} x f''(\eta), \\ &\bullet\ \frac{\partial^2 u}{\partial y^2} = a\sqrt{\frac{a}{\nu}} x f'''(\eta) \frac{\partial \eta}{\partial y} = \frac{a^2}{\nu} x f'''(\eta), \\ &\bullet\ \frac{\partial N}{\partial x} = a\sqrt{\frac{a}{\nu}} h(\eta), \\ &\bullet\ \frac{\partial N}{\partial y} = a x \sqrt{\frac{a}{\nu}} h'(\eta) \frac{\partial \eta}{\partial y} = \frac{a^2}{\nu} x h'(\eta), \\ &\bullet\ \frac{\partial^2 N}{\partial y^2} = \frac{a^2 x}{\nu} h''(\eta) \frac{\partial \eta}{\partial y} = \frac{a^2 x}{\nu} h''(\eta) \sqrt{\frac{a}{\nu}} = \frac{a^2\sqrt{a}}{\nu\sqrt{\nu}} x h''(\eta). \end{aligned}\right\} \tag{3.9}$$

Using (3.7), (3.8) and (3.9) in Eq. (3.2), we have

$$
\begin{aligned}
& a^2x(f'(\eta))^2 - a^2xf(\eta)f''(\eta) = a^2x + \left(\frac{\mu+k}{\rho}\right)\left(\frac{a^2}{\nu}xf'''(\eta)\right) + \frac{k}{\rho}\left(\frac{a^2}{\nu}xh'(\eta)\right) \\
& \Rightarrow (f'(\eta))^2 - f(\eta)f''(\eta) = 1 + \left(\frac{\mu+k}{\nu\rho}\right)f'''(\eta) + \left(\frac{k}{\nu\rho}\right)h'(\eta) \\
& \Rightarrow \left(\frac{\mu+k}{\nu\rho}\right)f''' + ff'' + 1 - (f')^2 + \left(\frac{k}{\nu\rho}\right)h' = 0 \\
& \Rightarrow (1+K)f''' + ff'' + (1-f'^2) + Kh' = 0, \quad \left(\because\ \nu = \frac{\mu}{\rho} \text{ and } K = \frac{k}{\nu\rho}\right). \qquad (3.10)
\end{aligned}
$$

Using (3.6), (3.7) and (3.9) in (3.3), we have

$$
\begin{aligned}
& \rho j\left(a^2\sqrt{\frac{a}{\nu}}xf'h - \sqrt{a\nu}\,\frac{a^2}{\nu}xfh'\right) = \left(\mu+\frac{k}{2}\right)j\left(\frac{a^2}{\nu}\sqrt{\frac{a}{\nu}}xh''\right) \\
& \qquad\qquad - k\left(2a\sqrt{\frac{a}{\nu}}xh + a\sqrt{\frac{a}{\nu}}xf''\right) \\
& \Rightarrow \rho j\left(a\sqrt{\frac{a}{\nu}}f'h - \sqrt{a\nu}\,\frac{a}{\nu}fh'\right) = \left(\mu+\frac{k}{2}\right)j\left(\frac{a}{\nu}\sqrt{\frac{a}{\nu}}h''\right) - k\left(2\sqrt{\frac{a}{\nu}}h + \sqrt{\frac{a}{\nu}}f''\right) \\
& \Rightarrow \rho j\left(a\sqrt{\frac{a}{\nu}}f'h - \sqrt{a\nu}\left(\sqrt{\frac{a}{\nu}}\right)^2 fh'\right) = \left(\mu+\frac{k}{2}\right)j\left(\frac{a}{\nu}\sqrt{\frac{a}{\nu}}h''\right) \\
& \qquad\qquad - k\left(2\sqrt{\frac{a}{\nu}}h + \sqrt{\frac{a}{\nu}}f''\right) \\
& \Rightarrow \rho ja\,(f'h - fh') = \frac{a\mu}{\nu}\left(1+\frac{k}{2\mu}\right)jh'' - k\,(2h+f'') \\
& \Rightarrow f'h - fh' = \frac{\mu}{\rho\nu}\left(1+\frac{k}{2\mu}\right)h'' - \frac{k}{\rho ja}\,(2h+f'') \\
& \Rightarrow \left(1+\frac{K}{2}\right)h'' + fh' - f'h - K(2h+f'') = 0, \quad \left(\because\ K = \frac{k}{\mu} = \frac{k}{\nu\rho} \text{ and } j = \frac{\nu}{a}\right).
\end{aligned}
$$

(3.11)

To convert the boundary conditions (3.4) into the dimensionless form, the following procedure has been adopted.

- (a) $\quad y = 0 \Rightarrow \sqrt{\frac{\nu}{a}}\eta = 0 \Rightarrow \eta = 0.$ (3.12)

  (b) $\quad v = 0 \Rightarrow -\sqrt{a\nu} f(\eta) = 0 \Rightarrow f(\eta) = 0.$ (3.13)

  (c) $\quad u = u_w(x) + u_{slip} = bx + \left(A\frac{\partial u}{\partial y} + B\frac{\partial^2 u}{\partial y^2}\right)$ ([24])

  $$\Rightarrow \quad axf'(\eta) = bx + A\left(a\sqrt{\frac{a}{\nu}}xf''(\eta)\right) + B\left(\frac{a^2}{\nu}xf'''(\eta)\right)$$

  $$\Rightarrow \quad f'(\eta) = \frac{b}{a} + A\sqrt{\frac{a}{\nu}}f''(\eta) + B\frac{a}{\nu}f'''(\eta)$$

  $$\Rightarrow \quad f'(\eta) = \epsilon + \lambda f''(\eta) + \delta f'''(\eta). \tag{3.14}$$

  (d) $\quad N = -n\frac{\partial u}{\partial y} \Rightarrow a\sqrt{\frac{a}{\nu}}xh(\eta) = -n\left(a\sqrt{\frac{a}{\nu}}xf''(\eta)\right)$

  $$\Rightarrow \quad h(\eta) = -nf''(\eta). \tag{3.15}$$

- (a) $\quad y \to \infty \Rightarrow \sqrt{\frac{\nu}{a}}\eta \to \infty \Rightarrow \eta \to \infty.$ (3.16)

  (b) $\quad u \to u_e(x) \Rightarrow axf'(\eta) \to ax \Rightarrow f'(\eta) \to 1.$ (3.17)

  (c) $\quad N \to 0 \quad \Rightarrow a\sqrt{\frac{a}{\nu}}xh(\eta) \to 0 \Rightarrow h(\eta) \to 0.$ (3.18)

In (3.14), the stretching/shrinking rate has been represented by $\epsilon{=}\frac{b}{a}$, the first order slip represented by $\lambda{=}A\sqrt{\frac{a}{\nu}}$ and the second order slip by $\delta{=}B\frac{a}{\nu}$, where A and B have the following formulations [24]

$$\left.\begin{aligned} A &= \frac{2}{3}\left(\frac{3-\alpha l^3}{\alpha} - \frac{3}{2}\frac{1-l^2}{K_n}\right)\lambda, \\ B &= -\frac{1}{4}\left[l^4 + \frac{2}{K_n^2}\left(1+l^2\right)\right]\lambda^2. \end{aligned}\right\} \tag{3.19}$$

Thus, the dimensionless form of the mathematical model of the present problem is:

$$\left.\begin{aligned}(1+K)\,f'''+ff''+(1-f'^2)+Kh'=0,\\ \left(1+\frac{K}{2}\right)h''+fh'-f'h-K(2h+f'')=0,\end{aligned}\right\} \tag{3.20}$$

along with BCs:

$$\left.\begin{aligned}&f(0)=0,\quad f'(0)=\epsilon+\lambda f''(0)+\delta f'''(0),\\ &h(0)=-nf''(0),\quad f'(\eta)\longrightarrow 1,\quad h(\eta)\longrightarrow 1\ \text{ as }\ \eta\to\infty.\end{aligned}\right\} \tag{3.21}$$

3.3 Solution Methodology

The numerical solution of the mathematical model in the form of non-linear differential equations (3.20) along with the boundary conditions (3.21) was reported by Sharma *et al.* [38]. They opted the finite-difference method for the numerical solution of the above model. In the present section, shooting method has been proposed to reproduce the same solution. The Runge-Kutta technique of order four and the Newton's technique for solving the non-linear algebraic equations, are the main components of the shooting method. Let us re-write equation (3.20) as:

$$f'''=-\frac{1}{1+K}\left(ff''+Kh'+(1-f'^2)\right), \tag{3.22}$$

$$h''=\frac{2}{2+K}\left(f'h-fh'+K(2h+f'')\right). \tag{3.23}$$

To have a system of first order ODEs, use the notations:

$$f=y_1,\ f'=y_1'=y_2,\ f''=y_2'=y_3,\ h=y_4,\ h'=y_4'=y_5. \tag{3.24}$$

By using the notations (3.24), we have the following IVP:

$$\left.\begin{aligned}
y_1' &= y_2, & y_1(0) &= 0,\\
y_2' &= y_3, & y_2(0) &= s,\\
y_3' &= -\frac{1}{1+K}\left(y_1\ y_3 + (1-y_2^2) + Ky_5\right), & & \\
& & y_3(0) &= \frac{1}{\lambda}\left(s-\epsilon+\frac{\delta}{1+K}\left((1-s^2)+Kt\right)\right),\\
y_4' &= y_5, & y_4(0) &= \frac{-n}{\lambda}\left(s-\epsilon+\frac{\delta}{1+K}\left((1-s^2)+Kt\right)\right),\\
y_5' &= \frac{2}{2+K}\left(y_2\ y_4 - y_1y_5 + K\left(2y_4+y_3\right)\right), & y_5(0) &= t.
\end{aligned}\right\} \tag{3.25}$$

For the computational purpose, the unbounded domain $[0,\infty)$ has been replaced by a bounded domain $[0,\eta_\infty]$, where η_∞ is some suitable finite real number. It is chosen in such a way that the solutions of the problem start looking settled for $\eta > \eta_\infty$. In (3.25), the missing initial conditions s and t are to be chosen such that

$$y_2(\eta_\infty,\ s,\ t) - 1 = 0\ , \quad y_4(\eta_\infty,\ s,\ t) = 0. \tag{3.26}$$

To start the iterative process, choose $s = s_0$, $t = t_0$. To update the values of s and t, Newton's iterative scheme has been used.

$$\begin{pmatrix} s_{n+1} \\ t_{n+1} \end{pmatrix} = \begin{pmatrix} s_n \\ t_n \end{pmatrix} - \begin{pmatrix} \frac{\partial y_2}{\partial s} & \frac{\partial y_2}{\partial t} \\ \frac{\partial y_4}{\partial s} & \frac{\partial y_4}{\partial t} \end{pmatrix}^{-1}_{(s_n,\ t_n)} \begin{pmatrix} y_2(\eta_\infty,\ s_n,\ t_n) - 1 \\ y_4(\eta_\infty,\ s_n,\ t_n) \end{pmatrix} \tag{3.27}$$

To implement the Newton's scheme, consider the following notations:

$$\frac{\partial y_1}{\partial s} = y_6\ ,\ \frac{\partial y_2}{\partial s} = y_7, \ldots \frac{\partial y_5}{\partial s} = y_{10}, \tag{3.28}$$

$$\frac{\partial y_1}{\partial t} = y_{11}\ ,\ \frac{\partial y_2}{\partial t} = y_{12}, \ldots \frac{\partial y_5}{\partial t} = y_{15}. \tag{3.29}$$

Differentiating equations (3.25), first w.r.t. s and then w.r.t. t, we get the following fifteen first order ODEs along with the associated initial conditions.

$$
\left.
\begin{aligned}
y_6' &= y_7, & y_6(0) &= 0,\\
y_7' &= y_8, & y_7(0) &= 1,\\
y_8' &= -\frac{1}{1+K}\left(y_6y_3 + y_1y_8 - 2y_2y_7 + Ky_{10}\right), & & \\
& & y_8(0) &= \frac{1}{\lambda}\left[1 - \frac{2\delta s}{1+K}\right],\\
y_9' &= y_{10}, & y_9(0) &= \frac{-n}{\lambda}\left[1 - \frac{2\delta s}{1+K}\right],\\
y_{10}' &= \frac{2}{2+K}\left[y_7y_4 + y_2y_9 - y_6y_5 - y_1y_{10} + K\left(2y_9 + y_8\right)\right], & & \\
& & y_{10}(0) &= 0,\\
y_{11}' &= y_{12}, & y_{11}(0) &= 0,\\
y_{12}' &= y_{13}, & y_{12}(0) &= 0,\\
y_{13}' &= -\frac{1}{1+K}\left(y_{11}y_3 + y_1y_{13} - 2y_2y_{12} + Ky_{15}\right), & & \\
& & y_{13}(0) &= \frac{1}{\lambda}\left(\frac{\delta K}{1+K}\right),\\
y_{14}' &= y_{15}, & y_{14}(0) &= -\frac{n}{\lambda}\left(\frac{\delta K}{1+K}\right),\\
y_{15}' &= \frac{2}{2+K}\left[y_{12}y_4 + y_2y_{14} - y_{11}y_5 - y_1y_{15} + K\left(2y_{14} + y_{13}\right)\right], & & \\
& & y_{15}(0) &= 1.
\end{aligned}
\right\} \tag{3.30}
$$

Next, the IVP in the form of fifteen first order ODEs given in (3.25) and (3.30) is solved by the RK−4 method. If for a sufficiently small ϵ^*,

$$
max\ \{|y_2(\eta_\infty, s_n, t_n) - 1|,\ |y_4(\eta_\infty, s_n, t_n)|\} > \epsilon^*, \tag{3.31}
$$

the guessed values of s and t are updated by the Newton's iterative scheme:

$$
\begin{pmatrix} s_{n+1} \\ t_{n+1} \end{pmatrix} = \begin{pmatrix} s_n \\ t_n \end{pmatrix} - \begin{pmatrix} y_7 & y_{12} \\ y_9 & y_{14} \end{pmatrix}^{-1}_{(\eta_\infty,\ s_n,\ t_n)} \begin{pmatrix} y_2(\eta_\infty,\ s_n,\ t_n) - 1 \\ y_4(\eta_\infty,\ t_n,\ t_n) \end{pmatrix} \tag{3.32}
$$

The iterative process is repeated until, the following criteria is met.

$$max\ \{|y_2(\eta_\infty, s_n, t_n) - 1|,\ |y_4(\eta_\infty, s_n, t_n)|\} < \epsilon^*. \tag{3.33}$$

3.4 Results and Discussion

The main objective of the present section is to study the effect of different physical parameters like K (micro-polar parameter), λ (the first order slip parameter), ϵ (the stretching/shrinking rate), δ (the second order slip parameter) on the velocity and micro-rotation profiles. The present results have been compared with the previous results of Wang [40] and Bachok *et al.* [41] for different values of the stretching/shrinking rate ϵ in Table 3.1. Wang [40] and Bachok *et al.* [41] have discussed the stagnation point flow towards a stretching/shrinking sheet.

Values of ϵ	Wang [40]	Bachok *et al.* [41]	Current results
2.0	-1.88731	-1.8873066	-1.88730667
1.0	0	0	0
0.5	0.71330	0.7132949	0.71329496
0.0	1.232588	1.2325877	1.23258765
-0.25	1.40224	1.4022408	1.40224081
-0.5	1.49567	1.4956698	1.49566977
-1.0	1.32882	1.3288170	1.32881688
-1.2	0.55430	0.932473	0.93247336
-1.2465	–	0.5842956	0.58428274

TABLE 3.1: Comparison of $f''(0)$ for different values of ϵ. When $\lambda = 0$, $\delta = 0$, $K = 0$ and $n = 0.5$.

The impact of the first order slip λ on the velocity profile is presented in Figure 3.1 (a). By increasing the values of the λ, the velocity profile is increased. Physically, when slip occurs, the velocity of flow near the sheet is no longer equal to the stretching velocity of the sheet. Figure 3.2 (b) demonstrates the impact of first order slip λ on the velocity profile for different physical parameters. By increasing the values of λ, the velocity profile is decreased. Hence the boundary layer thickness is increased.

The variations in the micro-rotation profile for the λ are demonstrated in Figure 3.2 (a) and 3.2 (b). An opposite flow behavior is determined with the first and second solution. The thickness of boundary layer is deceased in the first solution and increases in the second solution.

Figures 3.3 (a) and 3.3 (b) demonstrate the impact of the second order slip parameter δ on the velocity profile. Figure 3.3(a) indicates that by increasing δ, the velocity profile is increased. Figure 3.3 (b) represents that by increasing δ, the velocity profile is reduced.

The variations in the microrotation profile for different values of the second order velocity slip δ are demonstrated in Figures 3.4 (a) and 3.4 (b). It shows that the microrotation profile is initially increased as δ is increased for the first solution and microrotation profile is decreased as δ is increased for the second solution.

The variations in the velocity profile for micropolar parameter K are demonstrated in Figures 3.5 (a) and 3.5 (b). By increasing the values of the micropolar fluid K, the velocity field is reduced in both the first and the second solution. It is evident from these Figure 3.5 (a) and 3.5 (b) that all curves approach the far field boundary conditions asymptotically.

The variations in the microrotation profile for micropolar parameter K are demonstrated in Figures 3.6 (a) and 3.6 (b). From these graphs, it can be observed that increasing the micropolar K, the velocity field is reduced in the lower half of the surface whereas it is enhanced in the upper half. The velocity is going to reduce initially with the mounting values of the micropolar K. The boundary layer thickness is increased in both the first and the second solution.

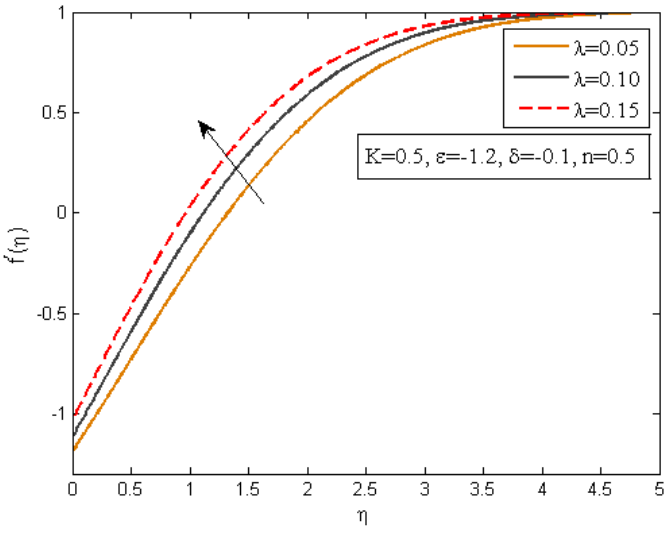

(a)

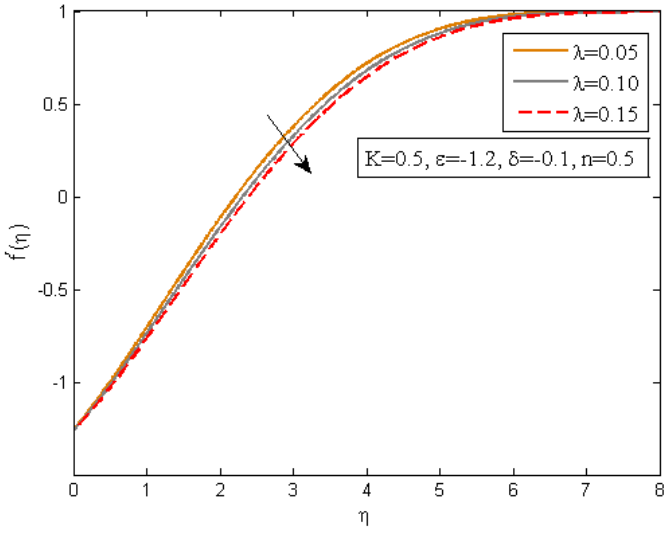

(b)

FIGURE 3.1: Influence of λ on f'.

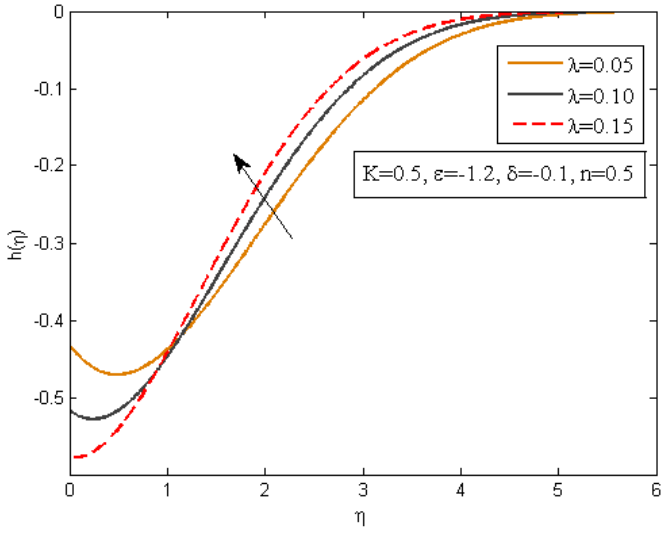

(a)

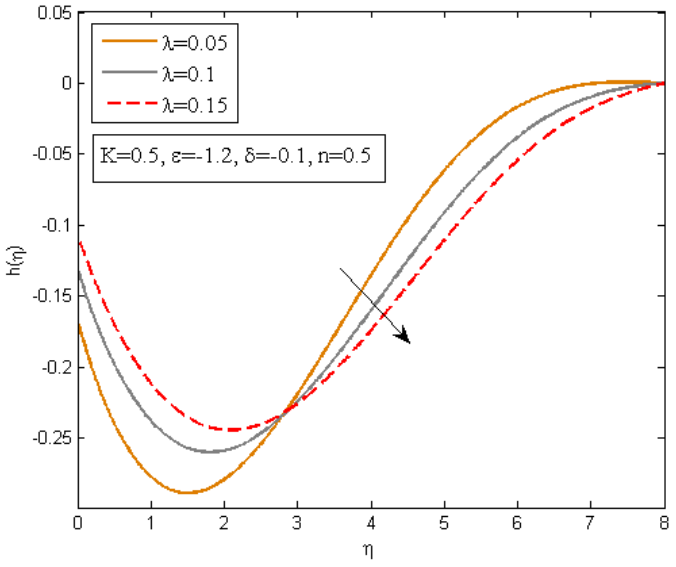

(b)

FIGURE 3.2: Influence of λ on h.

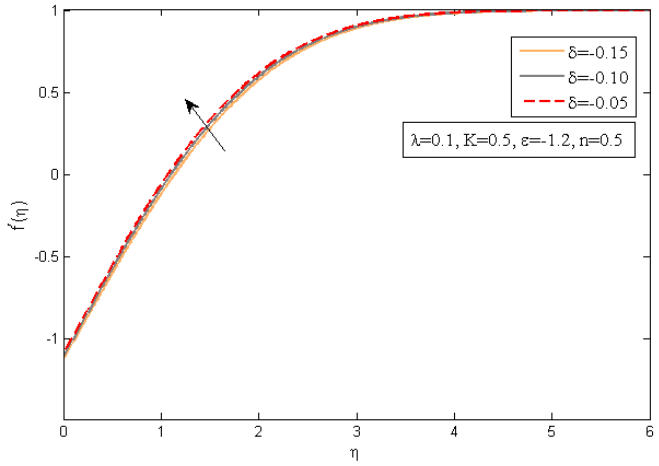

(a)

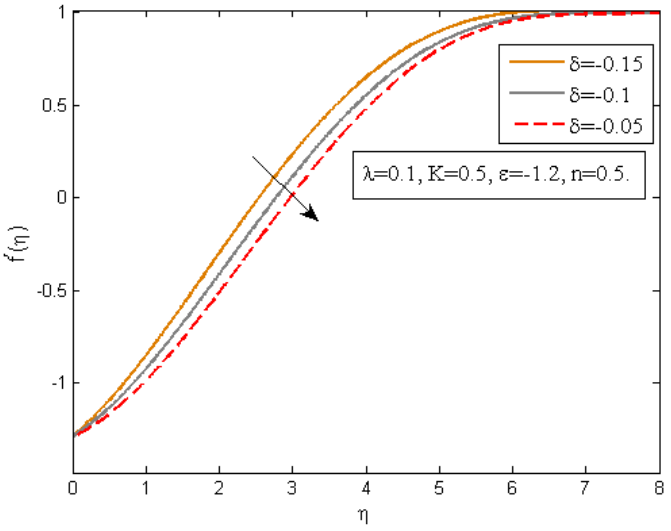

(b)

FIGURE 3.3: Influence of δ on f'.

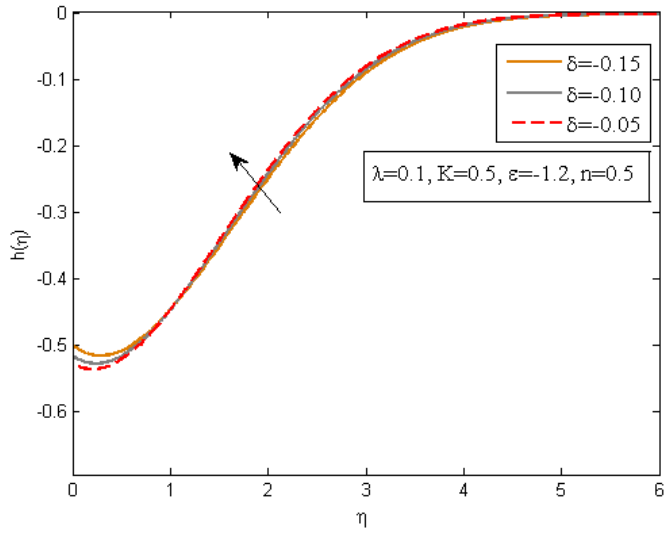

(a)

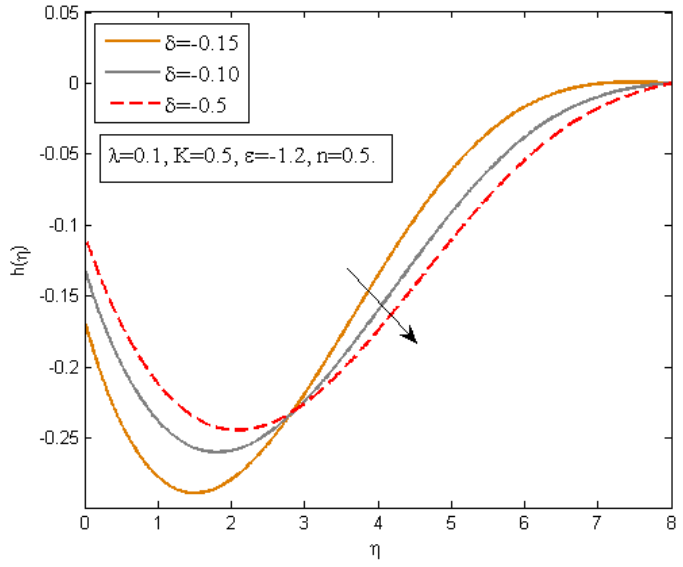

(b)

FIGURE 3.4: Influence of δ on h.

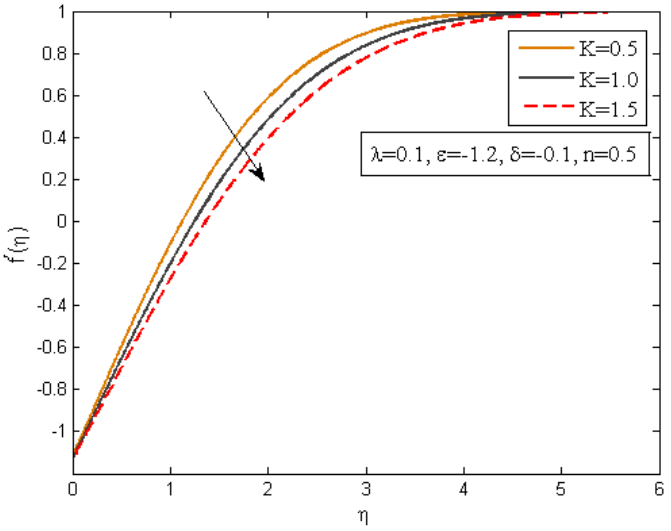

(a)

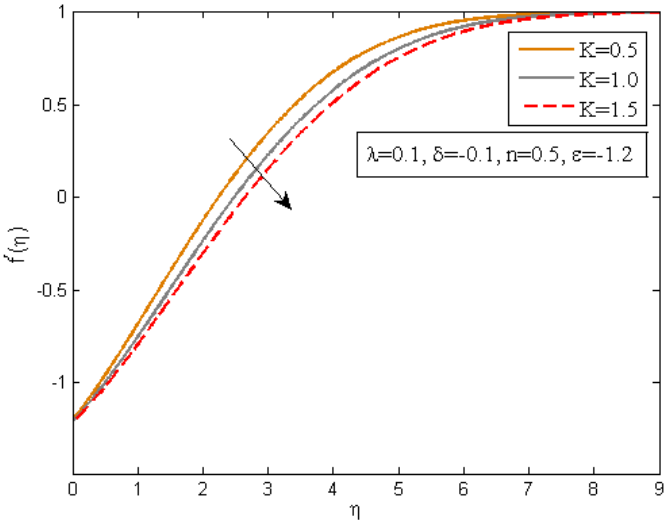

(b)

FIGURE 3.5: Influence of K on f'.

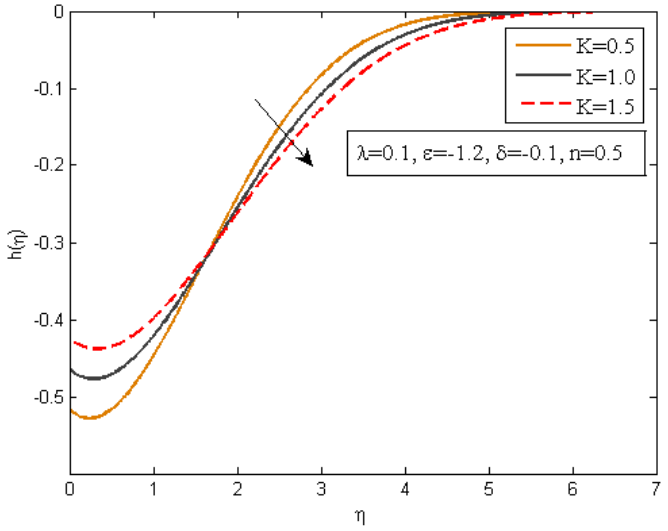

(a)

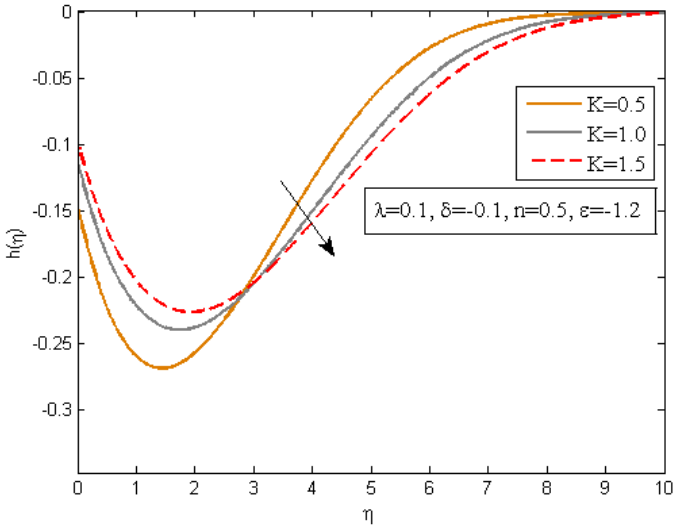

(b)

FIGURE 3.6: Influence of K on h.

Chapter 4

Thermal Radiation and MHD Micropolar Fluid over a Shrinking Sheet

4.1 Introduction

In the present chapter, the article of Sharma *et al.* [38] that was discussed in the previous chapter has been extended by considering the thermal radiation effect and the inclined MHD stagnation point flow of micropolar fluid due to stretching sheet. To convert the PDEs into the ODEs, the similarity transformation will be used. The numerical results have been found by the shooting technique using MATLAB. Finally, the numerical results are presented with a discussion of the effects of different physical parameters.

4.2 Mathematical Modeling

Consider a steady, two-dimensional stagnation point flow of an incompressible micropolar fluid on a stretching/shrinking sheet with the assumption of slip velocity effect. The free stream velocity has been represented by $u_e(x) = ax$ and the

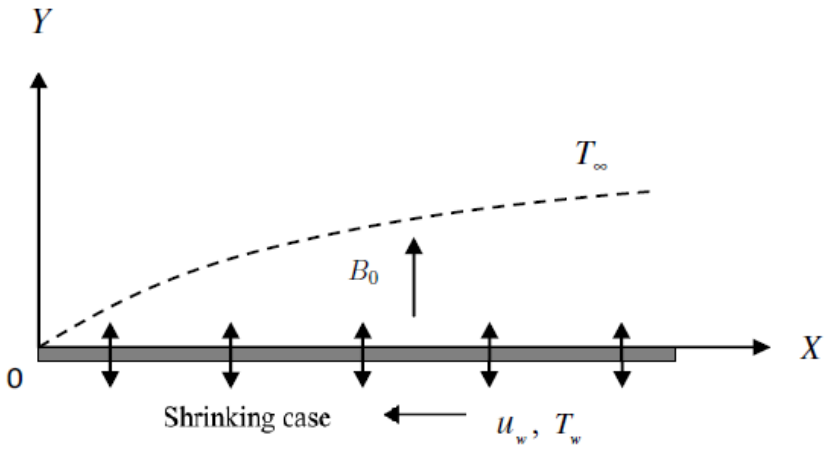

Figure 1: Geometry of the problem.

stretching/shrinking velocity by $u_w(x) = bx$. For the stretching sheet, b is taken positive whereas for the shrinking case, $b < 0$. The mathematical model of the flow, has been expressed as follows:

$$\frac{\partial u}{\partial x} + \frac{\partial v}{\partial y} = 0, \tag{4.1}$$

$$u\frac{\partial u}{\partial x} + v\frac{\partial u}{\partial y} = u_e\frac{\partial u_e}{\partial x} + \left(\frac{\mu + k}{\rho}\right)\frac{\partial^2 u}{\partial y^2} + \frac{k}{\rho}\frac{\partial N}{\partial y} - \frac{\sigma B_0^2}{\rho}\sin^2(\alpha)(u - u_e), \tag{4.2}$$

$$\rho j\left(u\frac{\partial N}{\partial x} + v\frac{\partial N}{\partial y}\right) = \left(\mu + \frac{k}{2}\right)j\frac{\partial^2 N}{\partial y^2} - k\left(2N + \frac{\partial u}{\partial y}\right), \tag{4.3}$$

$$u\frac{\partial T}{\partial x} + v\frac{\partial T}{\partial y} = \alpha_1\frac{\partial^2 T}{\partial y^2} - \frac{1}{\rho c_p}\frac{\partial q_r}{\partial y}, \tag{4.4}$$

where dynamic viscosity is denoted by μ, micro-rotation viscosity by k, fluid density by ρ, micro-inertia density by j, component of micro-rotation vector by N, fluid temperature by T, thermal diffusivity by α_1 and the radiative heat flux by q_r. The boundary conditions for the above equations are:

$$v = -V_s, \quad u_w(x) + u_{slip} = u, \quad N = -n\frac{\partial u}{\partial y}, \quad T = T_w \quad at \quad y = 0, \tag{4.5}$$

$$T = T_\infty, \quad u \to u_e(x), \quad N \to 0 \quad as \quad y \to \infty. \tag{4.6}$$

In the above equations, suction/injection is denoted by V_s, where V_s is greater than zero for suction velocity and less than zero for injection velocity. The slip

velocity has been represented by u_{slip}, the reference temperature by T_0 and ambient temperature by T_∞. Now, we use the following similarity variables.

$$\psi = \sqrt{\nu x u_e(x)} f(\eta) = \sqrt{a\nu} x f(\eta), \qquad \eta = \sqrt{\frac{u_e(x)}{\nu x}} y = \sqrt{\frac{a}{\nu}} y, \tag{4.7}$$

$$N = u_e(x)\sqrt{\frac{u_e(x)}{\nu x}} h(\eta) = a\sqrt{\frac{a}{\nu}} x h(\eta), \tag{4.8}$$

$$\theta(\eta) = \frac{T - T_\infty}{T_w - T_\infty} \Rightarrow T = \theta(\eta)\,(T_w - T_\infty) + T_\infty, \tag{4.9}$$

where the kinematic viscosity has been represented by ν and the stream function by ψ .

$$\left.\begin{aligned}
&\bullet \quad \frac{\partial T}{\partial x} = 0 \\
&\bullet \quad \frac{\partial T}{\partial y} = \theta'(T_w - T_\infty)\frac{\partial \eta}{\partial y} = \theta'(T_w - T_\infty)\sqrt{\frac{a}{\nu}}, \\
&\bullet \quad \frac{\partial^2 T}{\partial y^2} = \theta''(T_w - T_\infty)\sqrt{\frac{a}{\nu}}\frac{\partial \eta}{\partial y} = \theta''(T_w - T_\infty)\frac{a}{\nu}, \\
&\bullet \quad \frac{\partial T^4}{\partial y} = \frac{\partial}{\partial y}\left(T_\infty^4 + 4T_\infty^3(T - T_\infty)\right) \\
&\Rightarrow \frac{\partial T^4}{\partial y} = \frac{\partial}{\partial y}\left(T_\infty^4 + 4T_\infty^3\left(\theta(T_w - T_\infty) + T_\infty\right) - T_\infty\right) \\
&\Rightarrow \frac{\partial T^4}{\partial y} = 4T_\infty^3\theta'\left(T_w - T_\infty\right)\sqrt{\frac{a}{\nu}}, \\
&\bullet \quad q_r = -\frac{4\sigma^*}{3k^*}\frac{\partial T^4}{\partial y} = -\frac{16T_\infty^3\sigma^*}{3k^*}\theta'\left(T_w - T_\infty\right)\sqrt{\frac{a}{\nu}}, \\
&\bullet \quad \frac{\partial q_r}{\partial y} = -\frac{16T_\infty^3\sigma^*}{3k^*}\frac{\partial^2 T}{\partial y^2} \quad \because \frac{\partial^2 T}{\partial y^2} = \theta''\left(T_w - T_\infty\right)\frac{a}{\nu}.
\end{aligned}\right\} \tag{4.10}$$

Using (3.7), (3.8) and (3.9) from chapter. 3 in Eq. (4.2), we have

$$\begin{aligned}
a^2 x(f'(\eta))^2 - a^2 x f(\eta) f''(\eta) &= a^2 x + \left(\frac{\mu + k}{\rho}\right)\left(\frac{a^2}{\nu} x f'''(\eta)\right) + \frac{k}{\rho}\left(\frac{a^2}{\nu} x h'(\eta)\right) \\
&\quad - \frac{\sigma B_0^2}{a\rho}\sin^2(\alpha) a^2 x (f'(\eta) - 1) \\
\Rightarrow (f')^2 - f f'' &= 1 + \left(\frac{\mu + k}{\nu\rho}\right) f''' + \left(\frac{k}{\nu\rho}\right) h' - M\sin^2(\alpha)(f' - 1) \quad \because \quad M = \frac{\sigma B_0^2}{a\rho} \\
\Rightarrow \left(\frac{\mu + k}{\nu\rho}\right) f''' + f f'' + 1 - (f')^2 + \left(\frac{k}{\nu\rho}\right) h' - M\sin^2(\alpha)(f' - 1) &= 0 \\
\Rightarrow (1 + K) f''' + f f'' + (1 - f'^2) + K h' - (f' - 1) M\sin^2(\alpha) &= 0.
\end{aligned} \tag{4.11}$$

Using (3.7) and (3.9) in Eq. (4.3), we have

$$\rho j\left(a^2\sqrt{\frac{a}{\nu}}xf'h-\sqrt{a\nu}\,\frac{a^2}{\nu}xfh'\right)=\left(\mu+\frac{k}{2}\right)j\left(\frac{a^2}{\nu}\sqrt{\frac{a}{\nu}}xh''\right)-k\left(2a\sqrt{\frac{a}{\nu}}xh+a\sqrt{\frac{a}{\nu}}xf''\right)$$

$$\Rightarrow \rho j\left(a\sqrt{\frac{a}{\nu}}f'h-\sqrt{a\nu}\,\frac{a}{\nu}fh'\right)=\left(\mu+\frac{k}{2}\right)j\left(\frac{a}{\nu}\sqrt{\frac{a}{\nu}}h''\right)-k\left(2\sqrt{\frac{a}{\nu}}h+\sqrt{\frac{a}{\nu}}f''\right)$$

$$\Rightarrow \rho j\left(a\sqrt{\frac{a}{\nu}}f'h-\sqrt{a\nu}\left(\sqrt{\frac{a}{\nu}}\right)^2fh'\right)=\left(\mu+\frac{k}{2}\right)j\left(\frac{a}{\nu}\sqrt{\frac{a}{\nu}}h''\right)-k\left(2\sqrt{\frac{a}{\nu}}h+\sqrt{\frac{a}{\nu}}f''\right)$$

$$\Rightarrow \rho ja\left(f'h-fh'\right)=\frac{a\mu}{\nu}\left(1+\frac{k}{2\mu}\right)jh''-k\left(2h+f''\right)$$

$$\Rightarrow f'h-fh'=\frac{\mu}{\rho\nu}\left(1+\frac{k}{2\mu}\right)h''-\frac{k}{\rho ja}\left(2h+f''\right)$$

$$\Rightarrow \left(1+\frac{K}{2}\right)h''+fh'-f'h-K(2h+f'')=0,\quad \left(\because\ K=\frac{k}{\mu}\text{ and }j=\frac{\nu}{a}\right). \tag{4.12}$$

Using (4.10) in (4.4), we have

$$0-\theta'\left(T_w-T_\infty\right)af=\alpha_1\theta''\left(T_w-T_\infty\right)\left(\frac{a}{\nu}\right)+\frac{1}{\rho c_p}\frac{16T_\infty^3\sigma^*}{3k^*}\theta''\left(T_w-T_\infty\right)\left(\frac{a}{\nu}\right)$$

$$\Rightarrow -f\theta'=\frac{\alpha_1}{\nu}\theta''+\frac{4}{3\nu\rho c_p}\left(\frac{4T_\infty^3\sigma^*}{k^*}\theta''\right)$$

$$\Rightarrow -f\theta'=\left(\frac{1}{Pr}+\frac{4\alpha_1}{3\nu\rho c_p\alpha_1}\left(\frac{4T_\infty^3\sigma^*}{k^*}\right)\right)\theta''$$

$$\Rightarrow -f\theta'=\left(\frac{1}{Pr}+\frac{4\alpha_1}{3\nu k_1}\left(\frac{4T_\infty^3\sigma^*}{k^*}\right)\right)\theta''$$

$$\Rightarrow -f\theta'=\left(\frac{1}{Pr}+\frac{4Rd}{3Pr}\right)\theta''$$

$$-f\theta' Pr=\left(1+\frac{4Rd}{3}\right)\theta''\quad\left(\because\ Pr=\frac{\nu}{\alpha_1}\text{ and }Rd=\frac{4T_\infty^3\sigma^*}{k_1k^*}\right). \tag{4.13}$$

Now, include the following procedure for the conversion of (4.5) and (4.6) into the dimensionless form.

- $$y = 0 \Rightarrow \sqrt{\frac{\nu}{a}}\eta = 0 \Rightarrow \eta = 0. \tag{4.14}$$

$$v = V_s \Rightarrow -\sqrt{\nu a} f(\eta) = -V_s \Rightarrow f(\eta) = \frac{V_s}{\sqrt{\nu a}} \Rightarrow f(0) = \lambda_1. \tag{4.15}$$

$$u = u_w(x) + u_{slip} = bx + \left(A\frac{\partial u}{\partial y} + B\frac{\partial^2 u}{\partial y^2}\right)$$

$$\Rightarrow \quad axf'(\eta) = bx + A\left(a\sqrt{\frac{a}{\nu}}xf''(\eta)\right) + B\left(\frac{a^2}{\nu}xf'''(\eta)\right)$$

$$\Rightarrow \quad f'(\eta) = \frac{b}{a} + A\sqrt{\frac{a}{\nu}}f''(\eta) + B\frac{a}{\nu}f'''(\eta)$$

$$\Rightarrow \quad f'(\eta) = \epsilon + \lambda f''(\eta) + \delta f'''(\eta). \tag{4.16}$$

$$N = -n\frac{\partial u}{\partial y} \Rightarrow a\sqrt{\frac{a}{\nu}}xh(\eta) = -n\left(a\sqrt{\frac{a}{\nu}}xf''(\eta)\right)$$

$$\Rightarrow \quad h(\eta) = -nf''(\eta). \tag{4.17}$$

$$\theta(\eta) = \frac{T - T_\infty}{T_w - T_0} = \frac{T_w - T_\infty}{T_w - T_\infty} = 1. \tag{4.18}$$

- $$y \to \infty \Rightarrow \sqrt{\frac{\nu}{a}}\eta \to \infty \Rightarrow \eta \to \infty. \tag{4.19}$$

$$u \to u_e(x) \Rightarrow axf'(\eta) \to ax \Rightarrow f'(\eta) \to 1. \tag{4.20}$$

$$N \to 0 \quad \Rightarrow a\sqrt{\frac{a}{\nu}}xh(\eta) \to 0 \Rightarrow h(\eta) \to 0. \tag{4.21}$$

$$\theta(\eta) = \frac{T - T_\infty}{T_w - T_\infty} = \frac{T_\infty - T_\infty}{T_w - T_\infty} = 0. \tag{4.22}$$

Here $\lambda_1 = \frac{V_s}{\sqrt{\nu a}}$ is the suction/injection parameter, $\epsilon = \frac{b}{a}$ the stretching/shrinking rate, $\lambda = A\sqrt{\frac{a}{\nu}}$ the first order slip and $\delta = B\frac{a}{\nu}$ the second order slip. Thus, the dimensionless form of the mathematical model of the present problem is:

$$(1+K)f''' + ff'' + (1 - f'^2) + Kh' - (f' - 1)M\sin^2(\alpha) = 0, \tag{4.23}$$

$$\left(1 + \frac{K}{2}\right)h'' + fh' - f'h - K(2h + f'') = 0, \tag{4.24}$$

$$\left(1 + \frac{4Rd}{3}\right)\theta'' + f\theta' Pr = 0, \tag{4.25}$$

along with BCs::

$$f(0) = \lambda_1, \quad f'(0) = \epsilon + \lambda f''(0) + \delta f'''(0), \quad h(0) = -nf''(0), \quad \theta(0) = 1, \tag{4.26}$$

$$\theta(\eta) = 0, \quad f'(\eta) \to 1, \quad h(\eta) \to 0, \quad as \quad \eta \to \infty, \tag{4.27}$$

where magnetic field has been represented by M, the micropolar parameter by K, the Prandtl number by $Pr = \frac{\nu}{\alpha}$, the suction/injection by λ_1, the stretching/shrinking rate by ϵ, the aligned angle of magnetic field by α, the first order slip denotes by λ and the second order slip by δ. The skin friction coefficient and the local Nusselt number are expressed as

$$C_f = \frac{\tau_w + kN}{\rho u_e^2}, \qquad N_u = \frac{xq_w}{k(T - T_\infty)}, \tag{4.28}$$

where q_w, the heat flux and shear stress τ_w are expressed as

$$\tau_w = \left[(\mu + k)\frac{\partial u}{\partial y}\right]_{y=0}, \qquad q_w = -k\left[\left(1 + \frac{16\sigma^* T_\infty^3}{3k_1 k^*}\right)\frac{\partial T}{\partial y}\right]_{y=0}. \tag{4.29}$$

The dynamic viscosity has been represented by μ and the thermal diffusivity by k. By using (4.29) in (4.28), we get

$$C_f {Re_x}^{\frac{1}{2}} = [1 + (1 - n)K]f''(0), \qquad Nu_x {Re_x}^{-\frac{1}{2}} = -\left(1 + \frac{4Rd}{3}\right)\theta'(0). \tag{4.30}$$

4.3 Solution Methodology

The set of non-linear ODEs (4.23)-(4.25) along with the boundary conditions (4.26)-(4.27) can not be solved analytically. For this, we use a numerical technique i.e, the shooting method with four order Runge-Kutta method. Let us

re-write the equation(4.23)-(4.25) as:

$$f''' = \left(\frac{1}{1+K}\right)\left[M\sin^2(\alpha)(f'-1) - ff'' - Kh' - (1-f'^2)\right] \tag{4.31}$$

$$h'' = \left(\frac{2}{2+K}\right)[-fh' + f'h + K(2h + f'')] \tag{4.32}$$

$$\theta'' = \left(\frac{3}{3+4Rd}\right)(-f\theta' Pr) \tag{4.33}$$

For further proceeding, use the following notations:

$$f = y_1,\ f' = y_2,\ f'' = y_3,\ h = y_4,\ h' = y_5,\ \theta = y_6,\ \theta' = y_7. \tag{4.34}$$

By using the notations (4.34), we have the following IVP:

$$\left.\begin{aligned}
y_1' &= y_2,\\
y_2' &= y_3,\\
y_3' &= \left(\frac{1}{1+K}\right)\left[M\sin^2(\alpha)(y_2-1) - y_1\ y_3 - (1-y_2^2) - Ky_5\right],\\
y_4' &= y_5,\\
y_5' &= \left(\frac{2}{2+K}\right)\left[-y_1\ y_5 + y_2\ y_4 + K\,(2y_4 + y_3)\right],\\
y_6' &= y_7,\\
y_7' &= -y_1\ y_7\left(\frac{3Pr}{3+4Rd}\right),
\end{aligned}\right\} \tag{4.35}$$

along with the following initial conditions:

$$\left.\begin{aligned}
y_1(0) &= \lambda_1, \\
y_2(0) &= p, \\
y_3(0) &= \left(\frac{1+K}{(1+K)\lambda - \delta\lambda_1}\right) \\
&\quad \left[p - \epsilon - \delta\left(\frac{1}{1+K}\right)\left(M\sin^2(\alpha)(p-1) - Kt - (1-p^2)\right)\right], \\
y_4(0) &= \left(\frac{-n(1+K)}{(1+K)\lambda - \delta\lambda_1}\right) \\
&\quad \left[p - \epsilon - \delta\left(\frac{1}{1+K}\right)\left(M\sin^2(\alpha)(p-1) - Kt - (1-p^2)\right)\right], \\
y_5(0) &= t, \\
y_6(0) &= 1, \\
y_7(0) &= u,
\end{aligned}\right\} \tag{4.36}$$

where p, t and u are the initial guesses. In (4.36), the missing initial conditions p, t and u are to be chosen such that

$$y_2(\eta_\infty,\ p,\ t,\ u) - 1 = 0\ ,\quad y_4(\eta_\infty,\ p,\ t,\ u) = 0,\quad y_6(\eta_\infty,\ p,\ t,\ u) = 0. \tag{4.37}$$

To start the iterative process, choose $p = p_0$, $t = t_0$ and $u = u_0$. To update the values of p, t and u, Newton's iterative scheme has been used.

$$d^* = e^* - f^* g, \tag{4.38}$$

where

$$d^* = \begin{pmatrix} p_{n+1} \\ t_{n+1} \\ u_{n+1} \end{pmatrix},\quad e^* = \begin{pmatrix} p_n \\ t_n \\ u_n \end{pmatrix},\quad f^* = \begin{pmatrix} \frac{\partial y_2}{\partial p} & \frac{\partial y_2}{\partial t} & \frac{\partial y_2}{\partial u}, \\ \frac{\partial y_4}{\partial p} & \frac{\partial y_4}{\partial t} & \frac{\partial y_4}{\partial u}, \\ \frac{\partial y_6}{\partial p} & \frac{\partial y_6}{\partial t} & \frac{\partial y_6}{\partial u}, \end{pmatrix}^{-1}_{(\eta_\infty,\ p_n,\ t_n,\ u_n)},$$

$$g = \begin{pmatrix} y_2(\eta_\infty,\ p_n,\ t_n,\ u_n) - 1 \\ y_4(\eta_\infty,\ p_n,\ t_n,\ u_n) \\ y_6(\eta_\infty,\ p_n,\ t_n,\ u_n) \end{pmatrix}.$$

To run the Newton's scheme, consider the following notations:

$$\frac{\partial y_1}{\partial p} = y_8 \ , \ \frac{\partial y_2}{\partial p} = y_9, ... \frac{\partial y_7}{\partial p} = y_{14}, \tag{4.39}$$

$$\frac{\partial y_1}{\partial t} = y_{15} \ , \ \frac{\partial y_2}{\partial t} = y_{16} ... \ \frac{\partial y_7}{\partial t} = y_{21}, \tag{4.40}$$

$$\frac{\partial y_1}{\partial u} = y_{22} \ , \ \frac{\partial y_2}{\partial u} = y_{23}, ... \frac{\partial y_7}{\partial u} = y_{28}. \tag{4.41}$$

Differentiating equations (4.35) and (4.36) w.r.t. p, t and u, we get the following twenty eight first order ODEs along with the associated initial conditions.

$$y_8' = y_9, \qquad y_8(0) = 0, \tag{4.42}$$

$$y_9' = y_{10}, \qquad y_9(0) = 1, \tag{4.43}$$

$$y_{10}' = \frac{1}{1+K}\left(y_9 M \sin^2(\alpha) - y_8 y_3 - y_1 y_{10} + 2y_2 y_9 - K y_{12}\right),$$
$$y_{10}(0) = \frac{1+K}{(1+K)\lambda_1 - \delta\lambda_1}\left[1 - \frac{\delta}{1+K}\left(M\sin^2(\alpha) + 2p\right)\right], \tag{4.44}$$

$$y_{11}' = y_{12}, \qquad y_{11}(0) = \frac{-n(1+K)}{(1+K)\lambda_1 - \delta\lambda_1}\left[1 - \frac{\delta}{1+K}\left(M\sin^2(\alpha) + 2p\right)\right], \tag{4.45}$$

$$y_{12}' = \frac{2}{2+K}\left[-y_8 y_5 - y_1 y_{12} + y_9 y_4 + y_2 y_{11} + K\left(2y_{11} + y_{10}\right)\right],$$
$$y_{12}(0) = 0, \tag{4.46}$$

$$y_{13}' = y_{14}, \qquad y_{13}(0) = 0, \tag{4.47}$$

$$y_{14}' = \frac{3Pr}{3+4R_d}(-y_8 y_7 - y_1 y_{14}), \qquad y_{14}(0) = 0, \tag{4.48}$$

$$y_{15}' = y_{16}, \qquad y_{15}(0) = 0, \tag{4.49}$$

$$y_{16}' = y_{17}, \qquad y_{16}(0) = 0, \tag{4.50}$$

$$y_{17}' = \frac{1}{1+K}\left(y_{16} M \sin^2(\alpha) - y_{15} y_3 - y_1 y_{17} + 2y_2 y_{16} - K y_{19}\right),$$
$$y_{17}(0) = \frac{\delta K}{(1+K)\lambda_1 - \delta\lambda_1}, \tag{4.51}$$

$$y'_{18} = y_{19}, \qquad y_{18}(0) = \frac{-n\delta K}{(1+K)\lambda_1 - \delta\lambda_1}, \quad (4.52)$$

$$y'_{19} = \frac{2}{2+K}\left[-y_{15}y_5 - y_1y_9 + y_{16}y_4 + y_2y_{18} + K\left(2y_{18} + y_{17}\right)\right],$$

$$y_{19}(0) = 1, \quad (4.53)$$

$$y'_{20} = y_{21}, \qquad y_{20}(0) = 0, \quad (4.54)$$

$$y'_{21} = \frac{3Pr}{3+4R_d}(-y_{15}y_7 - y_1y_{21}), \qquad y_{21}(0) = 0, \quad (4.55)$$

and

$$y'_{22} = y_{23}, \qquad y_{22}(0) = 0, \quad (4.56)$$

$$y'_{23} = y_{24}, \qquad y_{23}(0) = 0, \quad (4.57)$$

$$y'_{24} = \frac{1}{1+K}\left(y_{23}M\sin^2(\alpha) - y_{22}y_3 - y_1y_{24} + 2y_2y_{23} - Ky_{26}\right),$$

$$y_{24}(0) = 0, \quad (4.58)$$

$$y'_{25} = y_{26}, \qquad y_{25}(0) = 0, \quad (4.59)$$

$$y'_{26} = \frac{2}{2+K}\left[-y_{22}y_5 - y_1y_{26} + y_{23}y_4 + y_2y_{25} + K\left(2y_{25} + y_{24}\right)\right],$$

$$y_{26}(0) = 0, \quad (4.60)$$

$$y'_{27} = y_{28}, \qquad y_{27}(0) = 0, \quad (4.61)$$

$$y'_{28} = \frac{3Pr}{3+4R_d}(-y_{22}y_7 - y_1y_{28}), \qquad y_{28}(0) = 1. \quad (4.62)$$

Next, the IVP in the form of twenty eight first order ODEs given in (4.35)-(4.36) and (4.42)-(4.62) is solved by the RK-4 method.

4.4 Results and Discussion

The main objective of the present section is to analyze the effect of different physical parameters such as micropolar K, magnetic field M, Prandtl number Pr, aligned angle of the magnetic field α, stretching/shrinking rate ϵ, first order slip λ, suction/injection λ_1, second order slip δ and the thermal radiation Rd on the

velocity, microrotation and temperature profiles. The numerical results have been shown in the form of tables and graphs.

In Table 4.1 and Table 4.2, display the impact of different physical parameters on local Nusselt number and skin-friction coefficient. We compare the obtained results by shooting technique with Matlab bvp4c and found both to be in excellent agreement. This Tables indicate that by increasing the micropolar parameter K, skin-friction coefficient is increased but the local Nusselt number is reduced. By increasing magnetic field M, the skin-friction coefficient is reduced and the local Nusselt number is enhanced. By increasing Prandtl number Pr , there is no effect on the skin-friction coefficient but the local Nusselt number is increased. Decrease in aligned angle of magnetic field, local Nusselt number and the skin-friction coefficient is decreased. Increase in microrotation parameter n and the stretching rate ϵ, the skin-friction coefficient is reduced but local Nusselt number is enhanced. By increasing second-order slip parameter δ, skin-friction coefficient is increased but local Nusselt number is reduced. By increasing first order slip parameter λ and suction parameter λ_1, skin-friction coefficient is decreased and the local Nusselt number is increased. Increase in thermal radiation Rd, there is no effect on the skin-friction coefficient but the local Nusselt number is reduced.

Figure 4.1 displays the effect of micropolar K on the velocity profile. This figure indicates that by increasing the micropolar parameter K, the velocity profile is reduced. Reverse flow is observed near the surface as the micropolar parameter K is increased. Figure 4.2 shows the effect of the micropolar parameter K on the micro-rotation profile. By increasing the micropolar parameter K, the microrotation profile is decreased in the lower half of the surface whereas it is enhanced in the upper half. The effect of K on the temperature profile is presented in Figure 4.3. By increasing K, the temperature profile is enhanced.

The variations in the velocity profile for different values of the magnetic field M are demonstrated in Figure 4.4. It can be seen that by increasing magnetic field M, the velocity profile is increased. This is due to the fact that the magnetic field M enhances the fluid motion in the boundary layer. Figure 4.5 shows the

variation in the micro-rotation profile for different estimations of the magnetic field M. By increasing M, the micro-rotation is increased. Thus, the boundary layer thickness is decreased. Figure 4.6 shows the effect of magnetic parameter M on the temperature profile. By increasing M, the temperature profile is reduced.

Figures 4.7 and 4.8 demonstrate the variations in the velocity and micro-rotation profiles for different estimations of the shrinking parameter ϵ. It is observed that by increasing the shrinking parameter ϵ, the velocity profile and micro-rotation profile is increased. Figure 4.9 shows the effect of the shrinking parameter ϵ on the temperature profile. By increasing ϵ, the temperature profile is reduced.

The suction parameter λ_1 effect on the velocity profile is presented in Figure 4.10. It can be seen that by increasing λ_1, the velocity profile is increasing significantly. The variations in the micro-rotation profile for λ_1 are demonstrated in Figure 4.11. From this graph, increasing λ_1, the micro-rotation profile is enhanced. The thickness of boundary layer is reduced. Figure 4.12 shows the impact of the suction parameter λ_1 on the temperature profile. By increasing λ_1, the temperature profile is decreased.

The variations in the temperature profile for different values of the Prandtl number Pr are demonstrated in Figure 4.13. It is observed that the greater Pr has weaker thermal diffusivity resulting in a low range temperature. Figure 4.14 shows the influence of Rd on the temperature profile. From this graph, by increasing Rd, the temperature profile is enhanced. Thus, the boundary layer thickness is increased.

K	M	Pr	α	n	δ	ϵ	λ	λ_1	Rd	shooting	bvp4c
0.5	0.2	0.5	$\pi/2$	0.5	-0.5	-1.2	0.5	0.2	0.5	1.57309	1.57495
1.2										1.94793	1.94515
2										2.30797	2.30618
3										2.68691	2.68620
	0.8									1.56460	1.56440
	2									1.51094	1.51292
	4									1.42251	1.42257
		0.6								1.57309	1.57495
		0.7								1.57309	1.57495
		0.8								1.57309	1.57495
			$\pi/6$							1.57360	1.57180
			$\pi/12$							1.57045	1.57033
			$\pi/18$							1.57034	1.56999
				0.6						1.51543	1.51557
				0.7						1.45533	1.45539
				0.8						1.39450	1.39451
					-1.8					0.86079	0.85989
					-1					1.21634	1.21699
					-0.05					1.93058	1.92862
						-1.9				2.04460	2.04407
						-1.7				1.92216	1.92162
						-1.5				1.78713	1.78638
							0.2			1.89263	1.89113
							0.3			1.77755	1.77533
							0.8			1.34207	1.34347
								0.4		1.57673	1.57660
								0.6		1.56611	1.56769
								0.8		1.54957	1.55107
									0.7	1.57309	1.57495
									0.9	1.57309	1.57495
									1.1	1.57309	1.57495

TABLE 4.1: Numerical results of $C_f(Re_x)^{1/2}$ for different values of K, M, α, n, δ, ϵ, λ and λ_1.

K	M	Pr	α	n	δ	ϵ	λ	λ_1	Rd	shooting	bvp4c
0.5	0.2	0.5	$\pi/2$	0.5	-0.5	-1.2	0.5	0.2	0.5	0.64744	0.64744
1.2										0.60581	0.60581
2										0.56310	0.56311
3										0.51637	0.51637
	0.8									0.68098	0.68099
	2									0.71478	0.71478
	4									0.74093	0.74091
		0.6								0.70554	0.70554
		0.7								0.75905	0.75906
		0.8								0.80897	0.80897
			$\pi/6$							0.63456	0.63458
			$\pi/12$							0.63097	0.63097
			$\pi/18$							0.63021	0.63022
				0.6						0.65405	0.65403
				0.7						0.66052	0.66051
				0.8						0.66687	0.66687
					-1.8					0.72746	0.72745
					-1					0.69222	0.69221
					-0.05					0.58035	0.58035
						-1.9				0.54107	0.54112
						-1.7				0.58218	0.58219
						-1.5				0.61224	0.61224
							0.2			0.58979	0.58981
							0.3			0.61432	0.61435
							0.8			0.67781	0.67781
								0.4		0.73216	0.73216
								0.6		0.81656	0.81655
								0.8		0.90088	0.90088
									0.7	0.70064	0.70065
									0.9	0.75090	0.75090
									1.1	0.79886	0.79886

TABLE 4.2: Numerical results of $Nu_x(Re_x)^{-1/2}$ for different values of K, M, Pr, α, n, δ, ϵ, λ, λ_1 and R_d.

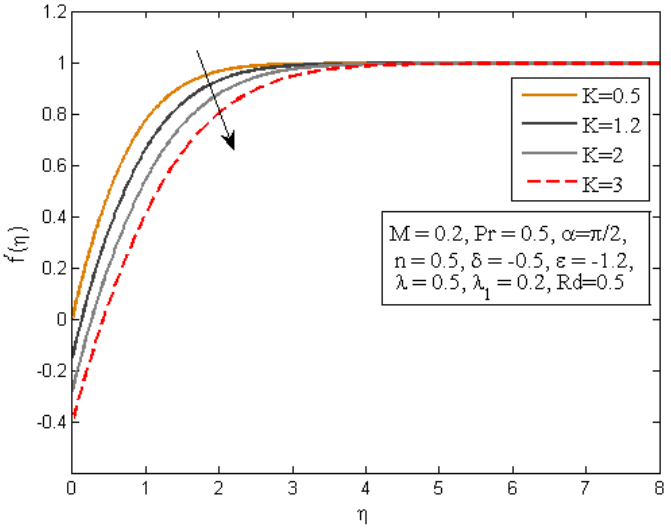

FIGURE 4.1: Impact of K on f'.

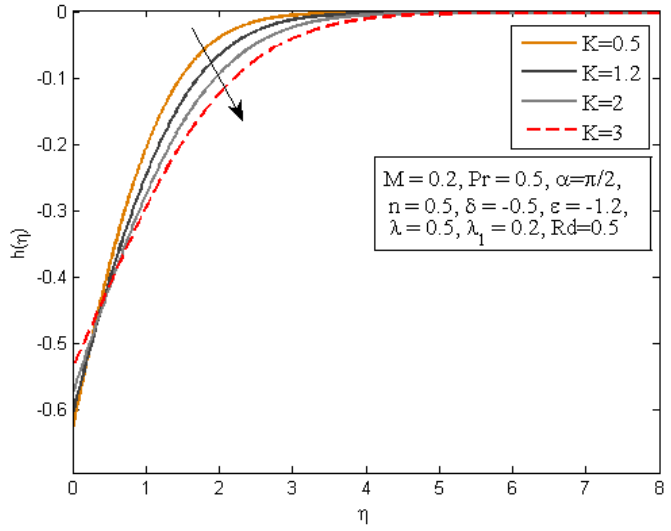

FIGURE 4.2: Impact of K on h.

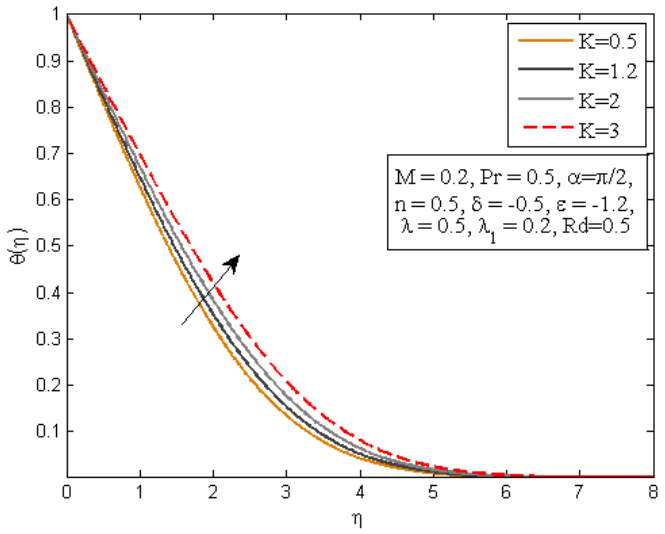

FIGURE 4.3: Impact of K on θ.

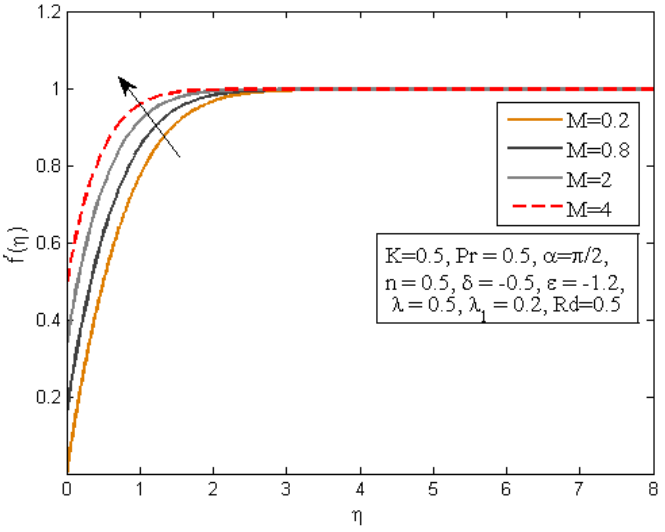

FIGURE 4.4: Impact of M on f'.

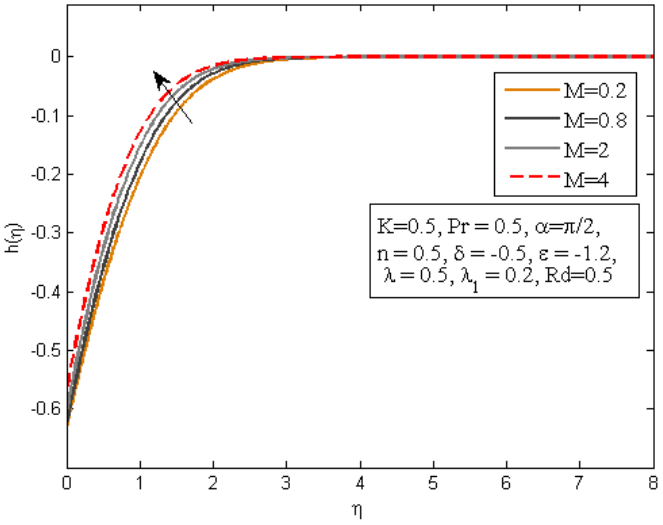

FIGURE 4.5: Impact of M on h.

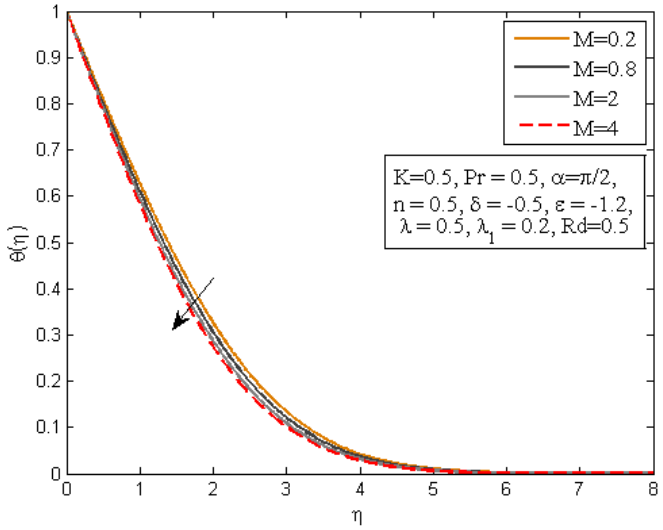

FIGURE 4.6: Impact of M on θ.

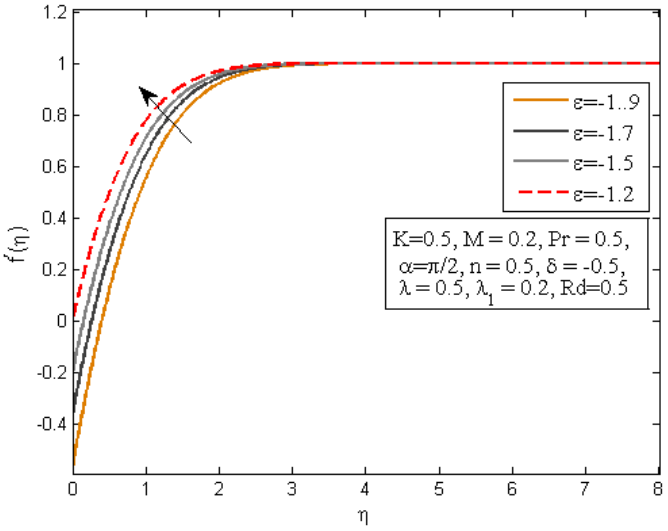

FIGURE 4.7: Impact of ϵ on f'.

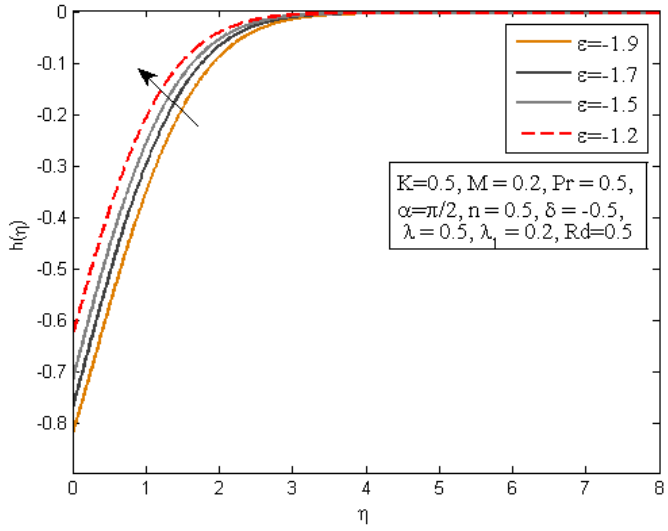

FIGURE 4.8: Impact of ϵ on h.

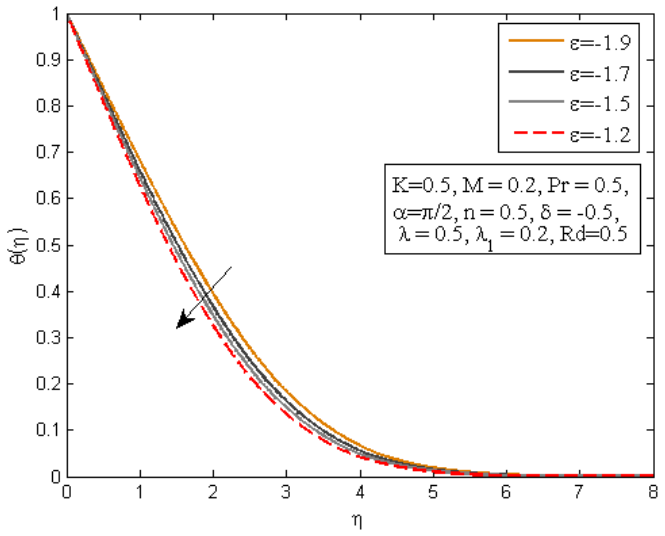

FIGURE 4.9: Impact of ϵ on θ.

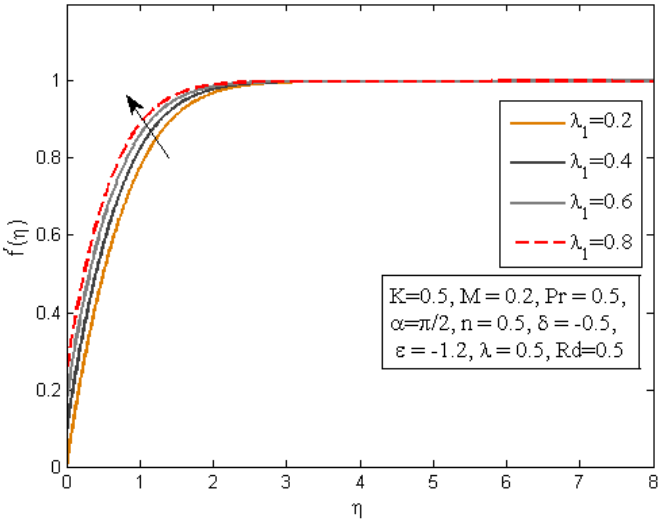

FIGURE 4.10: Impact of λ_1 on f'.

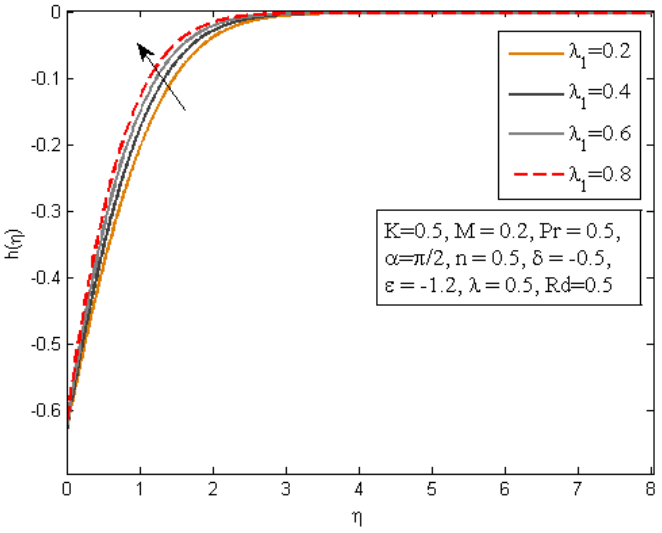

FIGURE 4.11: Impact of λ_1 on h.

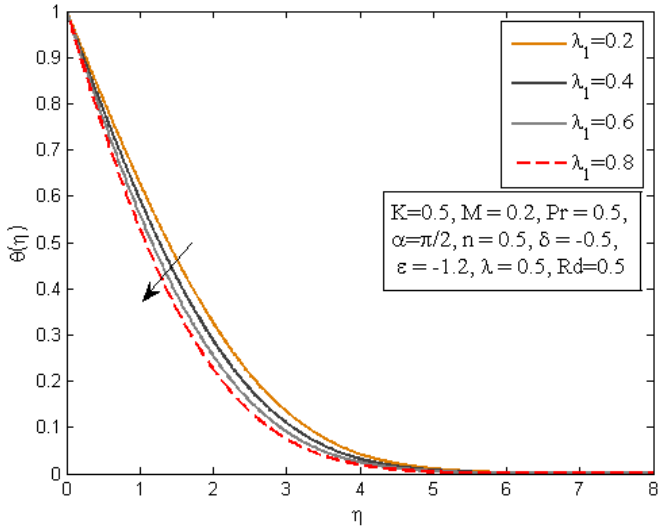

FIGURE 4.12: Impact of λ_1 on θ.

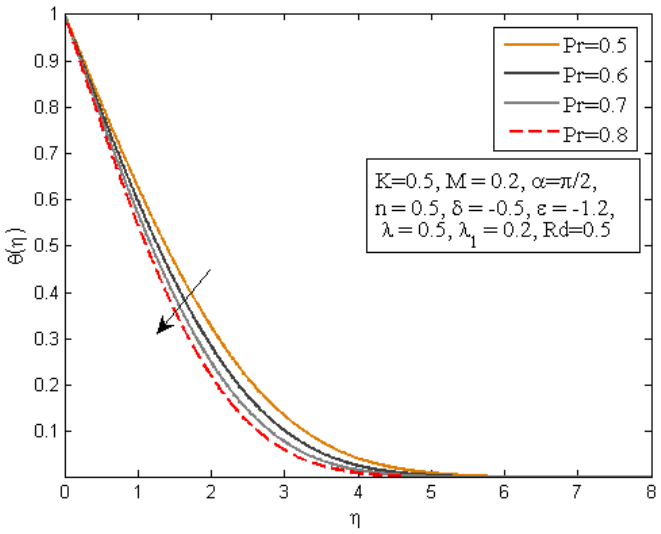

FIGURE 4.13: Impact of Pr on θ.

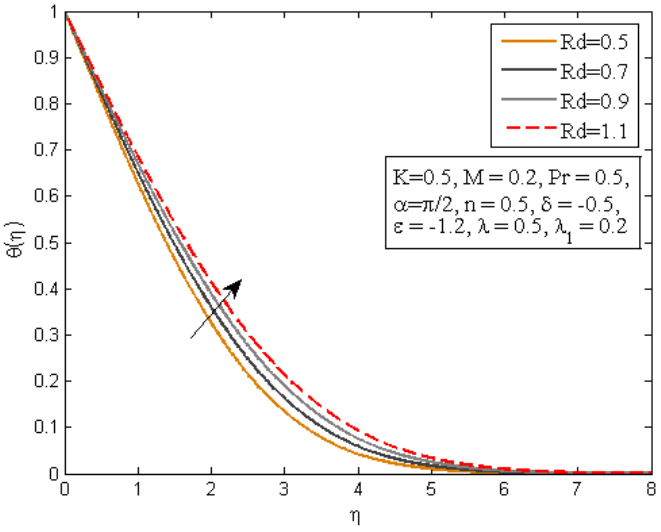

FIGURE 4.14: Impact of Rd on θ.

Chapter 5

Conclusion

In this thesis, we discussed the slip effect of a micropolar fluid over a stretching/shrinking sheet along with the thermal radiation and aligned magnetic field. The system of PDEs transformed into ODEs used by similarity transformation. The numerical results are found by the shooting technique in MATLAB. Significance of different physical parameters such as micropolar parameter K, magnetic field M, Prandtl number Pr, aligned angle of the magnetic field α, second order slip parameter δ, stretching/shrinking rate ϵ, first order slip λ, suction parameter λ_1 and the thermal radiation parameter Rd on the velocity, microrotation and temperature profiles are discussed tabularly and graphically.
Conclusions which are obtained:

• Increasing the micropolar parameter, the temperature profile is increased but the velocity and micro-rotation profiles are decreased.

• By increasing magnetic field, the velocity and microrotation profiles are increased and the temperature profile is decreased.

• Due to an increase in the shrinking parameter, temperature profile increases whereas the velocity and micro-rotation profiles are decreased.

• Increasing the suction parameter, the velocity and microrotation profiles are increased and temperature profile is reduced.

• By increasing the Prandtl number, the temperature profile is reduced. The thickness of boundary layer is decreased.

• Temperature profile increases with increase in thermal radiation.

5.1 Future Scope

In future, this problem may be extended in many directions focusing on the following ideas:

• The influence of viscous dissipation.

• The impact of Joule heating and heat generation and absorption.

Bibliography

[1] J. Thomason, P. Jenkins, and L. Yang, "Glass fibre strength—a review with relation to composite recycling," *Fibers*, vol. 4, p. 18, 2016.

[2] L. Zheng, J. Niu, X. Zhang, and Y. Gao, "MHD flow and heat transfer over a porous shrinking surface with velocity slip and temperature jump," *Mathematical and Computer Modelling*, vol. 56, pp. 133–144, 2012.

[3] B. C. Sakiadis, "Boundary-layer behavior on continuous solid surfaces: Laminar boundary-layer equations for two-dimensional and axisymmetric flow," *American Institute of Chemical Engineers*, vol. 7, pp. 6–28, 1961.

[4] A. Ishak, R. Nazar, and I. Pop, "Flow and heat transfer characteristics on a moving flat plate in a parallel stream with constant surface heat flux," *Heat and Mass Transfer*, vol. 45, pp. 563–567, 2008.

[5] K. Hiemenz, "The boundary layer on a straight circular zynder immersed in the uniform flow," *Dinglers J.*, vol. 326, pp. 321–324, 1911.

[6] E. Eckert, "The calculation of the heat transfer in the laminar boundary layer due to stretching sheet," *VDI Forschungsheft*, vol. 416, pp. 1–24, 1942.

[7] K. Zaimi and A. Ishak, "Stagnation-point flow towards a stretching vertical sheet with slip effects," *Mathematics*, vol. 4, p. 27, 2016.

[8] N. F. Fauzi, S. Ahmad, and I. Pop, "Stagnation point flow and heat transfer over a nonlinear shrinking sheet with slip effects," *Alexandria Engineering Journal*, vol. 54, pp. 929–934, 2015.

[9] K. Bhattacharyya, S. Mukhopadhyay, and G. C. Layek, "Slip effects on boundary layer stagnation-point flow and heat transfer towards a shrinking sheet," *International Journal of Heat and Mass Transfer*, vol. 54, pp. 308–313, 2011.

[10] A. C. Eringen, "Theory of micropolar fluids," *Journal of Mathematics and Mechanics*, pp. 1–18, 1966.

[11] T. T. N. D. Ariman, M. A. Turk, and N. D. Sylvester, "Applications of microcontinuum fluid mechanics," *International Journal of Engineering Science*, vol. 12, pp. 273–293, 1974.

[12] A. Ishak, R. Nazar, and I. Pop, "Mixed convection stagnation point flow of a micropolar fluid towards a stretching sheet," *Meccanica*, vol. 43, pp. 411–418, 2008.

[13] R. Bhargava, S. Sharma, H. S. Takhar, O. A. Bég, and P. Bhargava, "Numerical solutions for micropolar transport phenomena over a nonlinear stretching sheet," vol. 12, pp. 45–63, 2007.

[14] D. Rees and I. Pop, "Free convection boundary-layer flow of a micropolar fluid from a vertical flat plate," *IMA Journal of Applied Mathematics*, vol. 61, pp. 179–197, 1998.

[15] R. Nazar, N. Amin, D. Filip, and I. Pop, "Stagnation point flow of a micropolar fluid towards a stretching sheet," *International Journal of Non-Linear Mechanics*, vol. 39, pp. 1227–1235, 2003.

[16] A. Ishak, Y. Lok, and I. Pop, "Stagnation-point flow over a shrinking sheet in a micropolar fluid," *Chemical Engineering Communications*, vol. 197, pp. 1417–1427, 2010.

[17] T. Hayat, T. Javed, and Z. Abbas, "MHD flow of a micropolar fluid near a stagnation-point towards a non-linear stretching surface," *Nonlinear Analysis: Real World Applications*, vol. 10, pp. 1514–1526, 2009.

[18] N. A. Yacob, A. Ishak, and I. Pop, "Melting heat transfer in boundary layer stagnation-point flow towards a stretching/shrinking sheet in a micropolar fluid," *Computers & Fluids*, vol. 47, pp. 16–21, 2011.

[19] J. M. Dorrepaal, "Slip flow in converging and diverging channels," *Journal of engineering mathematics*, vol. 27, pp. 343–356, 1993.

[20] G. Bellani and E. A. Variano, "Slip velocity of large neutrally buoyant particles in turbulent flows," *New Journal of Physics*, vol. 14, p. 125009, 2012.

[21] C. Wang, "Analysis of viscous flow due to a stretching sheet with surface slip and suction," *Nonlinear Analysis: Real World Applications*, vol. 10, pp. 375–380, 2009.

[22] A. Noghrehabadi, R. Pourrajab, and M. Ghalambaz, "Effect of partial slip boundary condition on the flow and heat transfer of nanofluids past stretching sheet prescribed constant wall temperature," *International Journal of Thermal Sciences*, vol. 54, pp. 253–261, 2012.

[23] R. Sharma, A. Ishak, and I. Pop, "Partial slip flow and heat transfer over a stretching sheet in a nanofluid," *Mathematical Problems in Engineering*, 2013.

[24] L. Wu, "A slip model for rarefied gas flows at arbitrary Knudsen number," *Applied Physics Letters*, vol. 93, p. 253103, 2008.

[25] C. Wang and C.-O. Ng, "Stagnation flow on a heated vertical plate with surface slip," *Journal of heat transfer*, vol. 135, p. 074505, 2013.

[26] E. Fang, S. Yao, J. Zhang, and A. Aziz, "Viscous flow over a shrinking sheet with a second order slip flow model," *Communications in Nonlinear Science and Numerical Simulation*, vol. 15, pp. 1831–1842, 2010.

[27] M. M. Nandeppanavar, K. Vajravelu, M. S. Abel, and M. N. Siddalingappa, "Second order slip flow and heat transfer over a stretching sheet with nonlinear Navier boundary condition," *International Journal of Thermal Sciences*, vol. 58, pp. 143–150, 2012.

[28] R. Deissler, "An analysis of second-order slip flow and temperature-jump boundary conditions for rarefied gases," *International Journal of Heat and Mass Transfer*, vol. 7, pp. 681–694, 1964.

[29] A. V. Roşca and I. Pop, "Flow and heat transfer over a vertical permeable stretching/shrinking sheet with a second order slip," *International Journal of Heat and Mass Transfer*, vol. 60, pp. 355–364, 2013.

[30] M. Turkyilmazoglu, "Heat and mass transfer of MHD second order slip flow," *Computers & Fluids*, vol. 71, pp. 426–434, 2013.

[31] H. Alfvén, "Existence of electromagnetic-hydrodynamic waves," *Nature*, vol. 150, pp. 405–406, 1942.

[32] K. A. Yih, "Free convection effect on MHD coupled heat and mass transfer of a moving permeable vertical surface," *International Communications in Heat and Mass Transfer*, vol. 26, pp. 95–104, 1999.

[33] L. Zheng, J. Niu, X. Zhang, and Y. Gao, "MHD flow and heat transfer over a porous shrinking surface with velocity slip and temperature jump," *Mathematical and Computer Modelling*, vol. 56, pp. 133–144, 2012.

[34] O. D. Makinde and A. Ogulu, "The effect of thermal radiation on the heat and mass transfer flow of a variable viscosity fluid past a vertical porous plate permeated by a transverse magnetic field," *Chemical Engineering Communications*, vol. 195, pp. 1575–1584, 2008.

[35] M. Sheikholeslami, D. D. Ganji, M. Y. Javed, and R. Ellahi, "Effect of thermal radiation on magnetohydrodynamics nanofluid flow and heat transfer by means of two phase model," *Journal of Magnetism and Magnetic Materials*, vol. 374, pp. 36–43, 2015.

[36] A. Raptis, C. Perdikis, and H. S. Takhar, "Effect of thermal radiation on MHD flow," *Applied Mathematics and Computation*, vol. 153, pp. 645–649, 2004.

[37] A. Arpaci, "Effect of thermal radiation on the laminar free convection from a heated vertical plate," *International Journal of Heat and Mass Transfer*, vol. 11, pp. 871–881, 1968.

[38] R. Sharma, A. Ishak, and I. Pop, "Stagnation point flow of a micropolar fluid over a stretching/shrinking sheet with second-order velocity slip," *Journal of Aerospace Engineering*, vol. 29, p. 04016025, 2016.

[39] D. S. Kumar, "Fluid mechanics and fluid power engineering (SI Units)," p. 848, 2008.

[40] C. Wang, "Stagnation flow towards a shrinking sheet," *International Journal of Non-Linear Mechanics*, vol. 43, pp. 377–382, 2008.

[41] N. Bachok, A. Ishak, and I. Pop, "Melting heat transfer in boundary layer stagnation-point flow towards a stretching/shrinking sheet," *Physics letters A*, vol. 374, pp. 4075–4079, 2010.